COMPUTATIONAL MODELLING OF MOVEMENT OF WATER SOLUBLE POLLUTANTS IN THE SOIL

by

Eric Akowuah BSc. (Hons.)

A Thesis submitted to the Department of Mechanical Engineering,

Kwame Nkrumah University of Science and

Technology

in partial fulfillment of the requirements for the degree

of

MASTER OF SCIENCE

Department of Mechanical Engineering

College of Engineering

May 2011

DECLARATION

I hereby declare that this submission is my own work towards the MSc and that, to the best of my knowledge, it contains no material previously published by another person nor material which has been accepted for the award of any other degree of the University, except where due acknowledgment has been made in the text.

Eric Akowuah (PG2677708)	…….…...…………	………………….
Student Name & ID	Signature	Date

Certified by:

Dr. Joshua Ampofo	….………………….	……………….
Thesis Supervisor	Signature	Date

Certified by:

Prof. Francis K. Forson	…………………	……………….
Head of Department	Signature	Date

ABSTRACT

The thesis focuses on two dimensional modelling of water soluble pollutants through soil. Specifically, computational fluid dynamics (CFD) approach and adapted Navier-Stokes equations for porous flow are used to develop a code for flow of water soluble pollutants through fine sand. The code is used to simulate flow of water soluble pollutants in the soil within the laminar flow regime and to examine the distribution and dispersion of water soluble pollutants through soil layers. In developing the code, several flow equations and assumptions were considered and modified to suit the flow of water soluble pollutant through soil. Some of the equations incorporated in the simulation of the code include the Navier-Stokes equation, the Forchheimer equation and the Darcy's velocity equation among others. In addition, the code makes use of several flow variables such as Reynolds number and pressure difference. The code was validated qualitatively using an experimental set-up to monitor the flow of dye within a square area filled with fine sand for three different dye sources. The distribution and dispersion pattern of the dye used was then physically examined at various times as simulated in the program and the results compared. It was found that the concentration of the dye decreased qualitatively away from the source. This is evident from the physical observation of the dye colour configuration obtained at the end of all the experiments as it faded in a decreasing manner away from the source but qualitatively increased in concentration with time. All the flow patterns of the experiments were comparable to the simulated results. The code may be used to approximate, interpolate and extrapolate the concentration level of pollutants as well as the distance and time a pollutant could travel from a source within a computational domain.

TABLE OF CONTENT

Contents **Page**

LIST OF TABLES

LIST OF FIGURES

Figure **Page**

NOMENCLATURE

Symbol	Unit	Description
L	[m]	Characteristic length
Re	[ ]	Reynolds Number
ρ	[kgm^{-3}]	Density of fluid

ACKNOWLEDGEMENT

My foremost thanks goes to Almighty God for guiding me and giving me the strength and the potential to follow this path.

I am indebted to my Thesis Supervisor, Dr. Joshua Ampofo, for not only guiding me to face challenges of this dynamic and competitive world, but also his advice and immense contribution to this work.

In addition, my heartfelt gratitude also goes to my second Supervisor Dr. Y.A. Fiagbe of Mechanical Engineering Department and Mr. Emmanuel Adjei of Civil Engineering Department, KNUST for their support and contribution.

Moreover, my exceptional appreciation goes to my sweet Mother, Mrs. Abena Osaah for the best moral and financial support one could wish for.

Finally, I thank all friends, authors and persons who in one way or the other have helped and natured me academically to enable me come this far.

CHAPTER 1

INTRODUCTION

1.1 Background

Flow through and past porous media has attracted significant interest in recent years because of its importance in engineering and technology (Vafai, 2000). Researchers are still trying to understand some of the modeling aspects of flow through soils and other porous media. It is worth noting that most heuristic study of hydrogeology connected with the study of water flow pattern in the ground require the knowledge and continuous prediction of soil permeability changes and water flow direction.

Conventionally, tracers are widely used to study the behaviour of water flow in the soil and even beyond the ground water table so as to predict and or determine the direction and velocity of ground water movement. As used in hydrology, a tracer is matter or energy carried by water which will give information concerning the direction of flow and or velocity of the water as well as potential contaminants which could be transported by the water. Failures of tracer test are most commonly a result of incorrect choice of tracers, insufficient concentrations of tracers and a lack of an understanding of the hydrogeologic system being tested. Some of the most useful general tracers are bromide chloride, rhodamine WT, and various fluorocarbons.

However, in recent years most studies on water and pollutant flow patterns in the soil focuses on the use of computational models such as modflow (a three-dimensional finite-difference ground-water flow model by Michael G. Mcdonald and

Arlen W. Harbaugh in 1983) to estimate and or iterate the velocities of flow, direction of flow and contaminant levels. Studies of this nature use the soil and hydrogeological properties that has been experimentally determined as well as properties from existing theoretical models. Some of the prominent models are the Henry Darcy's law (1856) and the Forchheimmer equation (1901) for porous flow.

A peculiar problem associated with water flow in the soil and or groundwater which demands a continual quest for an answer, proper remediation as well as monitoring and control is the solubility and mobility of pollutants that are disposed into the soil. The porous nature of the soil enables pollutants to be conveyed from one locality to another with less resistance to movement of these pollutants. Such pollutant after an appreciable time (in months or years) would surely find their way into rivers, streams and groundwater which serve as the major source of drinking water for most rural dwellers.

In Ghana, a greater percentage of wastewater is illegally discharged directly into rivers and streams as well as the bare soil without treatment. Specifically, untreated sewage, poorly treated sewage, or overflow from under-capacity sewage treatment facilities can send water bearing-diseases into rivers and oceans. A typical incidence occurred in 2009 when an overflow of a cyanide containment pond of Anglogold Ashanti, Iduapriem Mine led to cyanide leakage into nearby rivers and forests. Lake Victoria, bordered by Kenya, Tanzania and Uganda has become a reservoir for excessive untreated effluents, including sewage, industrial waste and other chemicals. (IRIN News – August, 2008)

Mining companies in Ghana sometimes illicitly dump mining waste directly into rivers or other bodies of water as a method of disposal. Recently, the Wassa community near Tarkwa Gold Mine in September, 2009 complained about cyanide spillages as well as the release of other hazardous chemicals including arsenic, manganese, cadmium, iron, copper, and mercury, zinc and lead into water bodies through mining operation. Detail research by the Wassa Association of Communities Affected by Mining Changes (WACAM), revealed that River Nyam in Obuasi, which is a mining community had arsenic concentration of 13.56 as against 0.01 permissible levels required by the World Health Organization (WHO) and the Ghana Environmental Protection Agency (GEPA). (Public Agenda, 21st August, 2009) Moreover, physico-chemical parameters such as the pH; conductivity; turbidity and total dissolved solids were measured in all 400 water samples, made up of 200 from Obuasi and 200 from Tarkwa areas were collected between May and September 2008 using standard methods of analysis as prescribed by the American Water Works Association (AWWA, 1998) exceeded the World Health Organisation (WHO) and Ghana Environmental Protection Agency's (GEPA) permissible limits.

Mining causes water pollution in a number of ways. The mining process exposes heavy metals and sulfur compounds that were previously locked away in the earth. Rainwater leaches these compounds out of the exposed earth, resulting in "acid mine drainage" and heavy metal pollution that can continue long after the mining operations have ceased. Similarly, the action of rainwater on piles of mining waste transfers pollution to freshwater supplies. In the case of gold mining, cyanide is intentionally poured on piles of mined rocks to chemically extract the gold from the ore. Some of the cyanide ultimately finds its way into nearby water. Huge pools of mining waste which is known as "slurry" are often stored behind containment dams. If a dam leaks or bursts, water pollution is guaranteed.

Pollutants released from sources such as sewage sludge, waste liquids etc. are distributed throughout the soil system, while remaining in the soil solution as iron and organic and inorganic complexes some are mobile for uptake by plants (Hooda et al., 1997). This mobility and availability depends on several factor including soil porosity, soil texture and soil pH. Changes can occur in chemical form and mobility of metal in the leachate which are usually the result of variation in pH or reduction-oxidation (Sims and Patrick., 1978). Mobile forms of metals release from sludge, which are not taken up by plant root, may move down the profile and reach the water table. This pollution of ground water may affect surface water and possibly portable water supplies depending on the nature of aquifer configuration of an area.

Therefore, there is the need to study the flow pattern of water in the soil and possibly groundwater and surface water. Such study should try to mimic the flow structure of water in order to know where and when the associated pollution can be tolerated in a specified area of interest. Over the years, experimental research has been the tool for most studies until the recent introduction of computer modeling. Comparatively, computational modelling is a reliable and cheaper way of undertaking studies of this nature. It also provides the opportunity for inaccessible soil layers and rocks to be modeled as well as predicting the flow pattern of pollutants.

1.2 Scope of Study

This thesis focuses on using computational fluid dynamics (CFD) to analyse the flow of water and its associated pollutants in the ground. Computational fluid dynamics will be used to access the level of pollution and the results will be validated against soil samples from mining communities. This shall be achieved through the use of fluid flow properties and soil properties that relate to soil water dispersion. Experiments would be performed using soil samples for validation of CFD results. Moreover, existing data may also be used to validate subsequent simulation results.

1.3 Justification

In developing countries like Ghana, a great deal of wastewater is discharged indirectly or directly into rivers and streams and more often directly into the bare soil without proper treatment. This poses a serious threat to most inhabitants especially the rural folks whose major sources of drinking water are the rivers, lakes and streams as well as borehole water. Therefore, there is the need to develop a model that would simulate the flow pattern of contaminated water through the soil. Such a model may be utilized by city and town planners, borehole drillers and mining companies in their planning and operations.

1.4 Aim

The motive of this thesis is to simulate water flow pattern in the soil and examine the behaviour of water soluble pollutants.

1.5 Objectives

The aim can be achieved through the realization of the following objectives:

- Understanding soil water flow pattern and the associated pollution.
- To obtain a meaningful behavior of water flow in the ground which will be a useful material to mining centres, city planners and borehole drillers as well as policy makers on water flow and pollution.

1.6 Specific Objectives

- To determine the maximum distance and time a pollutant can travel given the necessary parameters of flow from a source.
- To simulate and compare the level of pollution from source and the haphazard travelling distances and times in an area.
- To obtain a reliable information for extrapolation and analysis of a new locality.

1.7 Methodology

The study will be undertaken to include the examination and analysis of the following:

1. Examine the basic properties of the soil and water flow:
    - Porosity of the different soil types, filter velocity of water through soil and the direction of surface and ground water movement. These are properties

that would help determine the type of flow regime in the soil. They would also serve as a guide in the determination of boundary conditions in the model. Knowing these also give a fair idea of a favourable flow equation to be used the computational model in order to achieve valid results.

- Soil Permeability Test. A test would be performed in Geotechnical Engineering Laboratory to determine the coefficient of permeability of the soil samples. This is a property of the medium of flow required for the modeling equations to be modified and used in the subsequent coding.

2. Review literature on flow through porous media and concurrently modify and adapt existing porous flow equations to model water movement through the soil.
3. Analysis of parameters using Computational Fluid dynamics (CFD):
   - Write algorithm connecting these parameters.
   - Coding of program with MATLAB.
4. Construction of physical model to obtain a realistic experimental results or data.
5. Validation of the results of CFD using experimental results or data and possibly existing data from the Environmental Department, Anglogold Ashanti, Obuasi, and Kumasi Metropolitan Assembly (KMA) and other recognized organizations just to ensure reliability.

1.8 Facilities Available

A well planned thesis must have reliable resources tools to enable the sets goals and aspirations become a reality. In the compilation of a thesis of this nature one has to be sure of some recognized facilities that would serve as a source of empowerment and a driving force for the commencement of the thesis. Notable among such facilities are the following:

1. Access to Mechanical engineering Computer Laboratory for current programs.
2. Availability of Environmental Science and Civil Engineering Departments for comprehensive and workable data for some validation.
3. Geotechnical Engineering Laboratory in the Civil Engineering Department.
4. Hydrology Section in the Civil Engineering Department.
5. Access to Fluid Laboratory in the Mechanical Engineering Department.
6. Access to Water and Sanitation Department in the Kumasi Metropolitan Assembly (KMA) for practical data which will aid in the validation process.
7. Access to Hydrology Department under the Ministry of Environment, Water and Sanitation in the Ashanti Region, Kumasi.
8. Availability of some data from the Environmental Department at Anglogold Ashanti, Obuasi for examination and validation.
9. Access to materials on fluid mechanics and computational fluid dynamics both from the Engineering Library and the Mini-libraries of some Lecturers.

CHAPTER 2

LITERATURE REVIEW

2.1 Flow Properties of the Soil and their Effect on Water Flow in the Soil

Generally, soil refers to the top few feet of the land surface. The soil acts as a natural filter to screen out many substances that mix with the water. But water will transport some contaminants into the groundwater. The amount of groundwater recharge, storage, discharge, as well as the extent of groundwater contamination, all depend on the soil properties. These include; texture, porosity, permeability, and attenuation capacity (soil's filtering ability)

2.1.1 Soil Profile

The soil profile gives a fair idea of the compositions of the soil layers in which water would maneuver its way from one point to another. Considering the different media of the profile, it is obvious that there is non-homogeneity. However, considering an infinitesimally small movement through a particular horizon, there is a somewhat close homogeneity because particles that are close and in the same horizon look alike.

2.1.2 Soil Texture

Soil is a mixture of three soil separates. These are; sands (the coarsest) , silts and clays (the finest). Classification of these separates is based on grain size. The following table shows the soil separate and its corresponding diameter size.

Table 2.1: Soil Grain Size

(Loxnachar et al, 2004.)

2.1.3 Porosity

The shape and arrangement of soil particles help determine porosity. Porosity or pore space is the amount of air space or void space between soil particles. Infiltration, groundwater movement, and storage occur in these void spaces. The porosity of soil or geologic materials is the ratio of the volume of pore space in a unit of material to the total volume of material. A mathematical equation of porosity is:

Porosity,

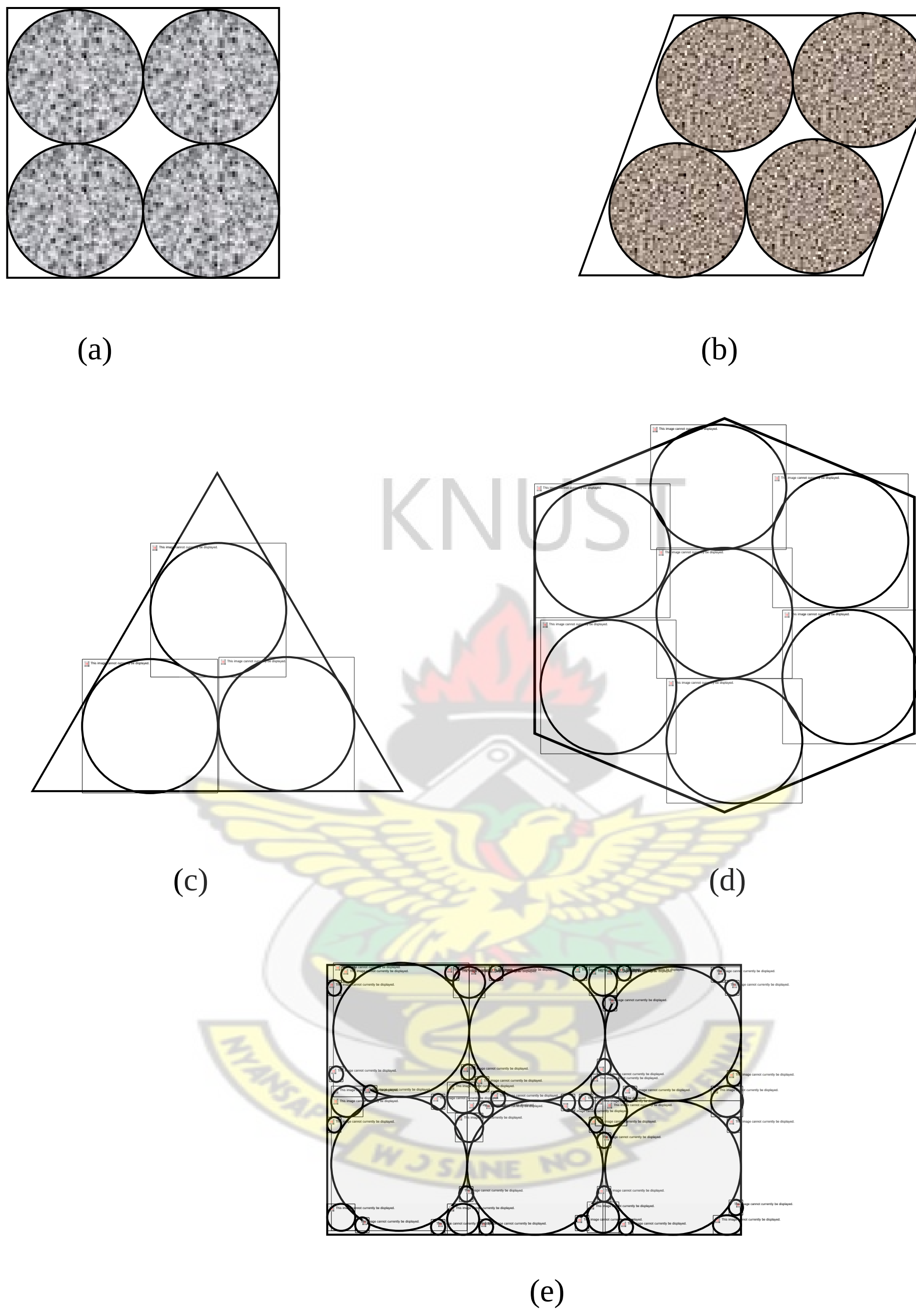

Figure 2.1: Different packing of soil particles in various shapes; (a) Cubic (b) Rhombohedral (c) Triangular (d) Hexagonal and (e) Cubic packing with smaller grains filling void spaces.

In Figure 2.1 below the particles stacked directly on top of each other (cubic packing) have higher porosity than the particles in a pyramid shape sitting on top of two other particles (rhombohedral packing). The difference between figure 2.1(e) and the (a) to (d) is that the smaller particles could fill in the void spaces between the larger particles, which would result in a lower porosity.

Not all particles are spheres or round. Particles exist in many shapes and these shapes pack in a variety of ways that may increase or decrease porosity. Generally, a mixture of grain sizes and shapes, results in lower porosity. The diameter size of the grain does not affect porosity. But porosity is a ratio of void space to total volume. A room full of ping pong balls would have the same porosity as a room full of basketballs, as long as the packing or arrangement is similar. Sands have large pore spaces, whereas clays have many small pore spaces. However, both sand and clay may have high porosity.

Table 2.2: Porosity Ranges for Sediments

Material	**Porosity (%)**
well-sorted sand or gravel	25-50
sand and gravel, mixed	20-35
glacial till	10-20
Silt	35-50
Clay	33-60

(MacCary and Lambert, 1962)

2.1.4 Filtering Capability of the Soil

Soil properties such as depth, texture, and permeability help determine the rate of groundwater recharge, as well as protection from groundwater contamination. Land surface factors such as topography, geology, and vegetation along with soil properties determine the potential for groundwater contamination. The soil acts as a natural filter. Moreover, filtration means more than capturing solid particles. Filtration also means retaining chemicals or dissolved substances on the soil particle surface, transforming chemicals through microbial or biological processing, and retarding movement of substances. The soil's ability to lessen the amount of or reduce the severity of groundwater contamination is called soil attenuation. “During attenuation, the soil holds essential plant nutrients for uptake by agronomic crops, immobilizes metals that might be contained in municipal sewage sludge, or removes bacteria contained in animal or human wastes”.

However, the soil's ability to filter contaminants is limited. Contaminant attenuation in soils depends on water moving through the top two layers of soil (horizons A and B) at a rate that ensures maximum contact between the percolating water that contains contaminants and the soil particles. Deep medium and fine-textured soils are the best, whereas coarse-textured materials are the worst in terms of contaminant removal. In coarse materials like sand, water moves through rapidly, reducing contact between the water and soil particles.

2.1.5 Direction and Velocity of Water Movement in the Soil

Soil water moves from areas of higher elevation or higher pressure/hydraulic head (recharge areas) to areas of lower elevation or pressure(hydraulic) head. This is where the groundwater is released into streams, lakes, wetlands, or springs (discharge areas). The base flow of streams and rivers, which is the sustained flow between storm events, is provided by groundwater. The direction of groundwater flow normally follows the general topography of the land surface.

Groundwater moves extremely slowly; usually inches per day, whereas rivers move more swiftly (feet per second (ft/sec)). However, in the sandy soils of Central Wisconsin, groundwater moves more quickly, between 1-5 feet per day. Even at this rate, groundwater and substances dissolved in it may take 5 years to travel about 1 mile In comparison, a small twig moving downstream in a river at about 1-2 ft/sec would only take about 1 hour to travel 1 mile.

2.2 Permeability

The size of pore space and interconnectivity of the spaces help determine permeability, so shape and arrangement of grains play a role. Permeability is a measure of a soil's or rock's ability to transmit a fluid, usually water. Often the term hydraulic conductivity is used when discussing soil water, groundwater and aquifer or soil layer properties. Hydraulic conductivity simply assumes that water is the fluid moving through a soil or rock type. Water can permeate between granular void or pore spaces, and fractures between rocks. The larger the pore space, the more permeable the material. However, the more poorly sorted a sample (mixed grain sizes), the lower the permeability because the smaller grains fill the openings created by the larger grains. The most rapid water and air movement is in sands and strongly aggregated soils, whose aggregates act like sand grains and pack to form many large pores.

On the other hand, clay has low permeability due to small grain sizes with large surface areas, which results in increased friction. Also these pore spaces are not well connected. Clay often creates confining layers in the subsurface. In rocks with fractures, the size of the openings, degree of interconnectedness, and the amount of open space all help determine permeability

The value of the permeability K_s has an enormous range: from about 1 m/s for gravels (i.e. 10^0 m/s), down to 10^{-9} to 10^{-10} m/s for clays – that's a range of 10 orders of magnitude (the permeability of clay is maybe 10,000,000,000 times less than that of gravel).

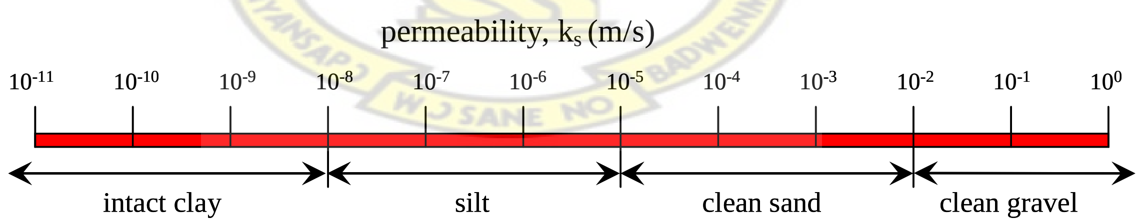

Figure 2.2: Scale Showing the Range of Permeability Values.

Table 2.3: Permeability for Sediments

Material	Permeability or Hydraulic Conductivity (cm/s)
well-sorted gravel	10^{-2} to 1
well-sorted sands, glacial outwash	10^{-3} to 10^{-1}
Silty sands, fine sands	10^{-5} to 10^{-3}
silt, sandy silts, clayey sands, till	10^{-6} to 10^{-4}
Clay	10^{-9} to 10^{-6}

(C. W. Fetter)

2.2.1 Permeability Model

The parameter that describes how easy or difficult it is for water to flow through soil is correctly called the hydraulic conductivity, but more commonly is called the permeability (k). This is analogous to thermal conductivity for heat flow in solids, or electrical conductivity for electrical current flow. The inverse of conductivity is resistivity. Flow of water in soils occurs in response to a difference in total head between two points or more precisely, it occurs in response to a gradient in total head, with flow being “down gradient” in the direction of reducing total head.

Figure 2.3 gives the definition of total head. What it says is that fluid flow depends on both the pressure in the water, and the elevation of the point above some arbitrary datum. In order to combine these two, the most convenient is to express the pressure at a point as pressure head (h_p), which can be thought of as “the height that water would rise to in a standpipe (tube) inserted into the soil to that point". Since this height has units of metres, it can be combined directly with the elevation head (h_e), which also has units of metres, to give total head (h_t).

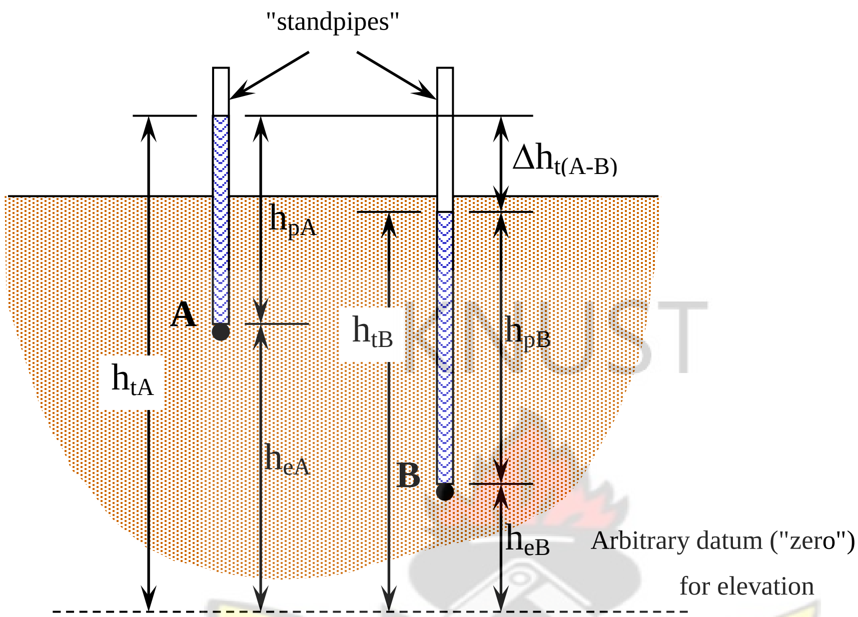

Figure 2.3: Definition of elevation head, pressure head and total head.
(Prof. Martin Fahey, University of Western Australia)

Though the water pressure at B is greater than at A (h_{pB} is greater than h_{pA}), the total head at A is greater than at B, so flow would tend to be from A to B. The hydraulic gradient between A and B is :

$$i = \Delta h_{t(A-B)}/L_{A-B.} \tag{2.2}$$

Thus, flow occurs in direction of reducing total head.

2.2.2 Relationship Between Permeability and Grading

The permeability depends primarily on pore size (more than on total pore volume, or void ratio e). In fact, void ratio per se is a very poor indicator of permeability – gravel, which could have a void ratio as low as 0.3, has permeability many orders of magnitude greater than soft clay, which could have a void ratio of well over 1.0. Many empirical relationships exist for estimating permeability from grain size. The best known (but not the only one) is Hazen's formula, which relates permeability to the smallest 10% of the soil (i.e. to $D_{10)}$ is:

$$k(mm/s) = C_k (D_{10})^2 \qquad (2.3)$$

Where D_{10} is given in mm and C_k is chosen from the table below:

Table 2.4: Hazen's Coefficient of permeability, C_k

C_k ($s^{-1}.mm^{-1}$)	Soil type	D_{10} range (mm)
8 – 12	Uniform sands	0.06 – 3.0
5 – 8	Well-graded sands and silty sands	0.003 – 0.6

The range of values given indicates the range of uncertainty. This is an empirical formula, obtained by correlating one property (C_k) against another (D_{10}^2), and the scatter in the data was probably very large.

2.2.3 Permeability Depends on Packing

For any particular soil, the permeability depends not just on the grading, but also on how 'dense' is the soil packing (i.e. on the void ratio, e). Thus, particular sand with a 'dense' packing might have a permeability value an order of magnitude lower than the same sand in a 'loose' packing.

2.2.4 Isotropic and Anisotropic Permeability

Many natural sedimentary soil deposits consist of sand with thin clay or silt layers, or clay with thin sand layers. The layering is generally horizontal (or nearly so). In these cases, flow occurring in a horizontal direction involves parallel flow, whereas flow in the vertical direction involves series flow.

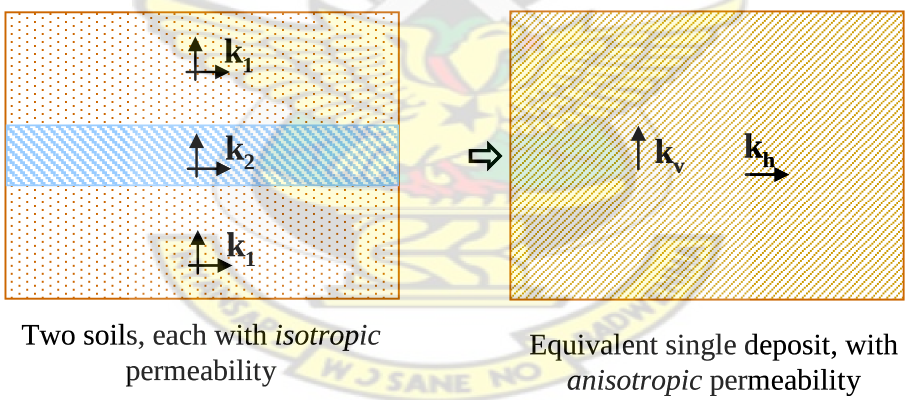

Figure 2.4: Isotropic and Anisotropic Permeability of Soil.

The presence of the thin layer within the thick one has completely different effect depending on whether flow is vertical or horizontal. In these cases, the equivalent overall permeability for vertical flow is the vertical permeability k_v, and that for horizontal flow is the horizontal permeability k_h.

2.3 Darcy's Law

Figure 2.4 shows a circular container, with cross sectional area A, containing sand of uniform density ("packing"), confined between two mesh screens, at a distance L apart. The total head loss from M to N is

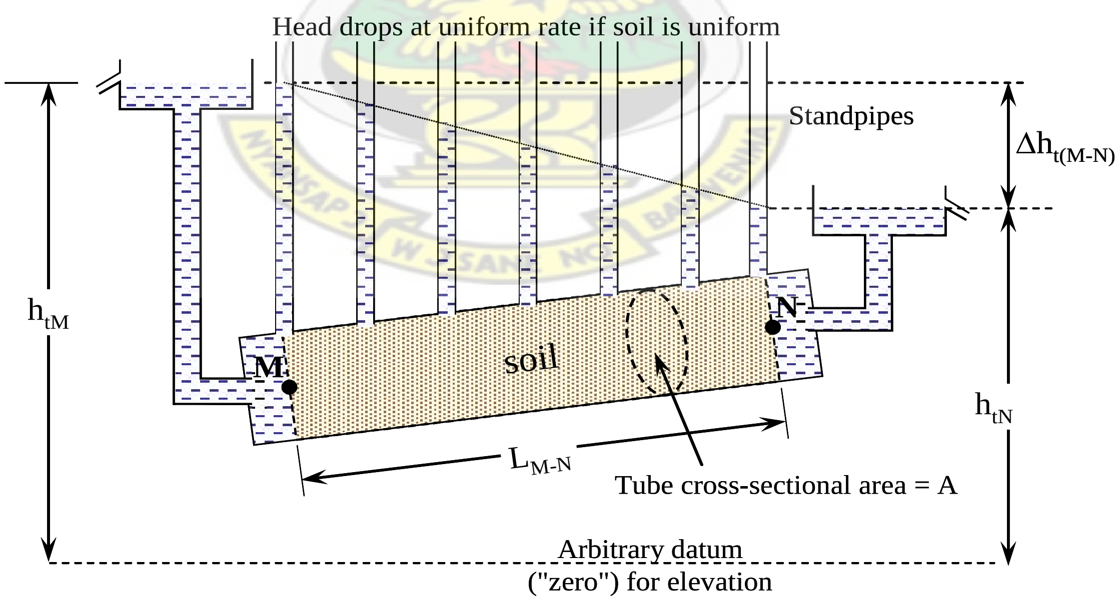

Dividing both sides by A, end up with Q/A on the left-hand side. This has units of m/s, and represents the average water velocity v through the tube if there was no soil present. Darcy's law can be re-stated as:

$$v = ki \qquad (2.9)$$

This is called the "Darcy velocity", or "apparent velocity", because it assumes that flow occurs across the total cross-sectional area (it ignores the fact that there is soil present). The true velocity or seepage velocity is given as:

$$\frac{v_s}{v} = \frac{A_T}{A_v} = \frac{1+e}{e} \quad \text{or} \quad v_s = \frac{1+e}{e} \cdot v$$

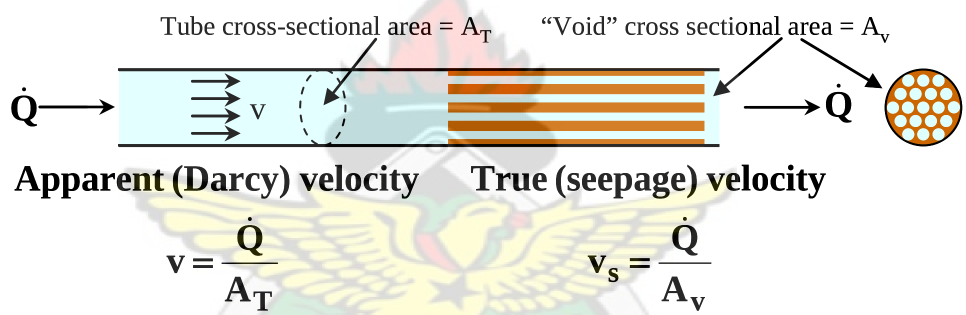

Figure 2.6: Schematic Difference between Apparent velocity and True velocity

2.3 Water Soluble Pollutant

Groundwater not only contains the hydrogen and oxygen atoms that form water (H_2O), but it also contains naturally dissolved gases from the atmosphere and dissolved minerals and gases from the soil and rock through which it passes. The soil filters the water and absorbs and removes many contaminants though some will pass through unimpeded. But if the soil layer is thin and has high permeability, or if the water table is close to the land surface, then the soil is less likely to adequately treat contamination.

The excess contaminants may pass through the zone of aeration and enter the groundwater in the zone of saturation. If this happens, a plume forms. A plume is an underground pattern of contaminant concentrations created by the movement of groundwater beneath a contaminant source. The contaminant spreads mostly laterally in the direction of groundwater movement. The site of original contamination has the highest concentration of contaminant and the concentration decreases as it moves further away from the source.

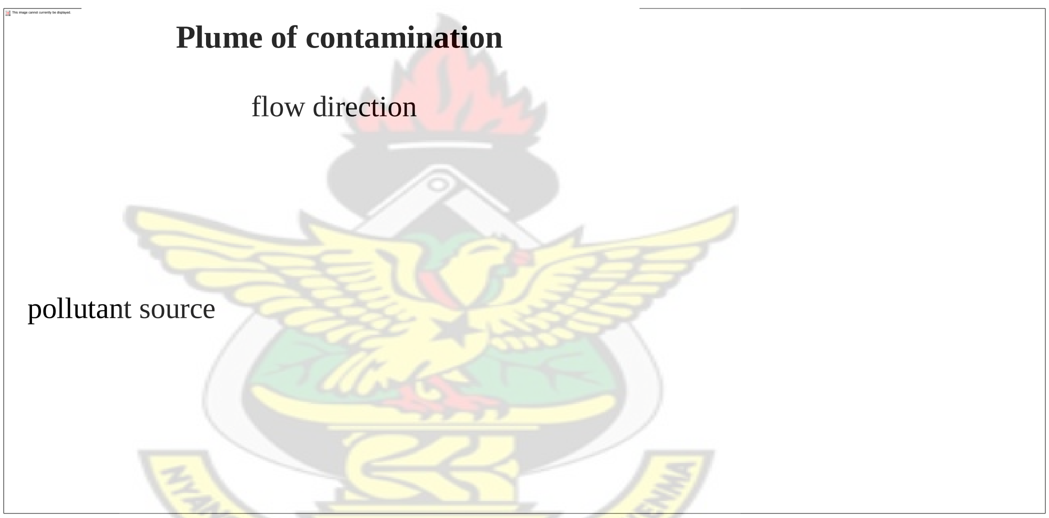

Figure 2.7: Direction of Pollutant Movement (Modified from C.W. Fetter)

Table 2.5: A Partial List of Human Sources of Groundwater Contaminants

Potential Groundwater Contamination Sources			
Municipal	**Industrial**	**Agricultural**	**Individual**
• air pollution • municipal waste land spreading • streets & parking lots • landfills • leaky sewer lines  	• air pollution • chemicals: storage & spills • fuels: storage & spills • mine tailing piles • pipelines • underground storage tanks 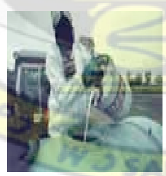 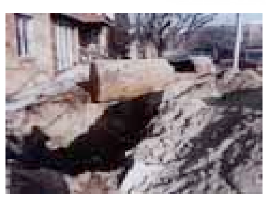	• air pollution • chemical spills • fertilizers • livestock waste storage facilities & land spreading • pesticides • underground storage tanks • wells: poorly constructed or abandoned  	• air pollution • fertilizers • homes • cleaners • detergents • motor oil • paints • septic systems • wells: poorly constructed or abandoned 

(Simmons Environmental Services, Inc., 2006.)

2.4 The States of Water

Gaseous, liquid and solid states of water may possibly co-exist in the soil where there is a time dependent temperature gradient for water which will vary slightly from one point to another. A quantity of water moving through the soil (both saturated and unsaturated zones) may exist in three states due to the influence of internally or externally generated thermal energy in the soil as follows:

1. A greater proportion as liquid at temperature above 273.16K (0^0C).
2. A minute proportion as a gas in the form of water vapour at a temperature close to 373K ($100\ ^0$C) and above.
3. Negligible proportion as an ice (solid) in some rare and special cases like the Antarctic parts of the earth.

CHAPTER 3

DEVELOPMENT OF A COMPUTATIONAL MODEL FOR WATER FLOW IN THE SOIL

3.1 Introduction

In developing a feasible model for water flow in the soil, a wide range of considerations and assumptions must be realized. There exist several flow equations and a careful selection and modification of these equations shall lead to the achievement of a justifiable model. The computational model, when well approached would give a close correlation between computed, experimental and or real life values.

3.2 Assumptions

This section further explicate on the assumptions that are essential and fundamental to the development of the flow model. These assumptions are sometimes stated in the literature review, though in many instances they are generally assumed. It may seem that these assumptions are too restrictive or too many, but they are less than the implicit assumptions commonly made. All additional assumptions made during the derivation of the equations would be clearly stated.

3.2.1 Assumptions Relating to Water

Assumption One: Water is incompressible and hence its density work is mainly concerned with horizontal and vertical gradual movement of water, these changes are comparatively insignificant. At a soil particle's surface the density difference of the liquid-liquid and the liquid-solid is relatively large, but it is assumed that the liquid adhered to the soil particle's surface does not contribute to the flow.

Assumption Two: The dynamic viscosity

3.2.2 Assumptions Regarding the Porous Medium

Assumption five: The porous medium of the different soil compositions within an averaging or control volume are considered homogeneous.

The soil profile gives a fair idea of the compositions of the medium in which water would maneuver its way from one point to another. Considering the different media (horizons) of the profile, it is obvious that there is non-homogeneity. However, considering an infinitesimally small movement through a particular horizon, there is a somewhat close homogeneity just because particles that are close and in the same horizon look alike.

Assumption six: The porosity of the soil is considered isotropic such that there is no natural direction associated with the pore structure inside a control volume.

Unconsolidated porous media are often isotropic within a specific layer. Due to natural deposition and sedimentation patterns, a layered porous medium is anisotropic. Here it is assumed that modeling takes place within an isotropic layer.

Assumption seven: Temperature of the soil compositions is also constant. Thus, isothermal condition is assumed.

Assumption eight: There is no deformation of the natural orientation of soil particles and its porosity.

Assumption nine: The reaction of various pollutants in the fluid with any chemical substance in the medium of flow is ignored.

3.2.3 Assumptions Regarding the Flow

Assumption ten: The dispersion of water in the soil is considered to be steady in nature and move in a uniform manner.

Assumption eleven: The flow is considered to turbulence free.

At turbulence flow regime, flow modeling becomes cumbersome since there is unclear behaviour of the fluid. Here, it is conveniently assumed that the flow through the soil shall remain in the laminar regime.

Assumption twelve: The flow is inertia free. Once stationary flow model is considered, the inertia term would be negligible and therefore could be neglected.

Assumption thirteen: The flow is assumed to be two-dimensional. All real life flows are in three-dimension but in this present work, it is assumed that water flows in a soil layer of unit thickness.

Assumption fourteen: Capillary force as well as adsorptive force is neglected.

3.3 The Navier-Stokes Equation for Incompressible Flow

One of the most reliable governing equations for two-dimensional incompressible flow used in computational fluid dynamics (CFD) is the Navier-Stokes Equation developed in 1845. *(John D. Anderson, Jr., Computational Fluid Dynamics, 1995)* . The two dimensional incompressible Navier-Stokes momentum equations in the non-conservative form and the continuity equation are given by:

3.4 Equations for Flow in a Porous Medium

To describe the motion of incompressible fluids in a medium, equations for continuity and that for the conservation of momentum are necessary. The Navier-Stokes equations for conservation of momentum are commonly used for flow in unrestricted medium. The Forchheimer equation is often used for stationary flow in a porous medium and may also be adapted for non-stationary flow by adding an inertia term.

Similarly, somehow averaged Navier-Stokes equation with extra terms that take the influence of the porous medium into account could be adapted to represent and suit the Forchheimmer equation for stationary flow. The continuity equation as well as the adapted two dimensional Navier-Stokes equations that describe the flow of incompressible fluids through a porous medium *(M.R.A. Van Gent (1992)* are given by:

3.5 Determination and Definition of Porous Flow and Geotechnical Parameters

The equations (3.4a) and (3.4b) mentioned above are in their generalized form and a critical study of each term and parameter would be required to substantiate their exact meanings. This section seeks to detail the various parameters that play significant role in the analysis of those equations.

3.5.1 The Filter Velocity

The velocity of a fluid in a porous medium is slower than free flow in an unrestricted medium. Consider a half-empty and half-porous tube conveying the same fluid from the frictionless, drag free and resistance free empty end of the tube where there is a smooth flow across the other portion of tube embedded with spherical soil particles. The spherical soil particles create pores in the second half of the medium making it porous. It obvious to identify that the velocity of the fluid in the first half of medium would be greater than that in the second half.

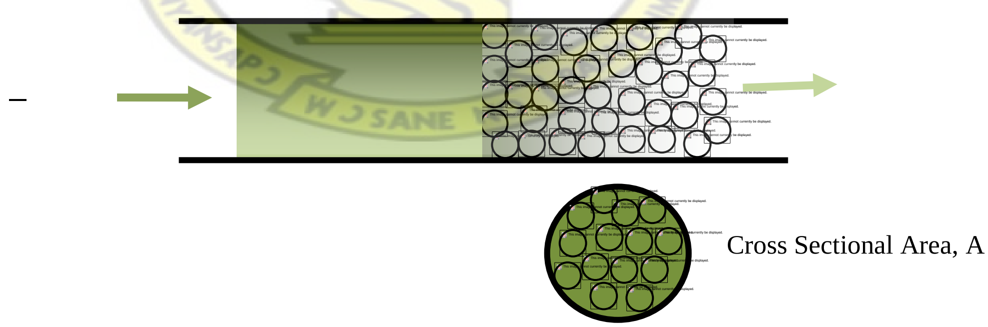

Figure 3.1: Illustration of filter and superficial velocity using a tube with half-filled soil.

The fluid flow rate through the tube is

depends on both the porosity and the density of the fluid as well as gravity. The relation between the intrinsic permeability, K and hydraulic conductivity or coefficient permeability, k as proposed by K.R. Rushton (2003), is expressed as:

- At any intermediate time, t the water level in the standpipe is given by *h* and its change with time is –

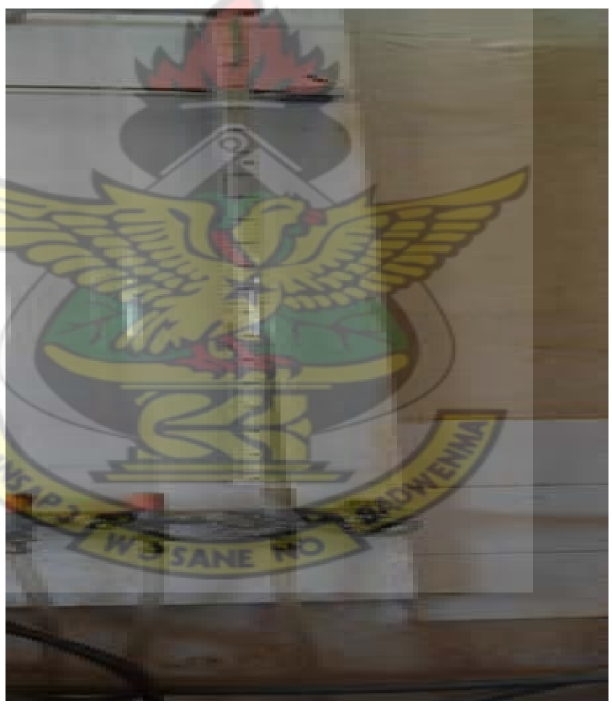

Figure 3.2: Experimental set-up to determine permeability of soil

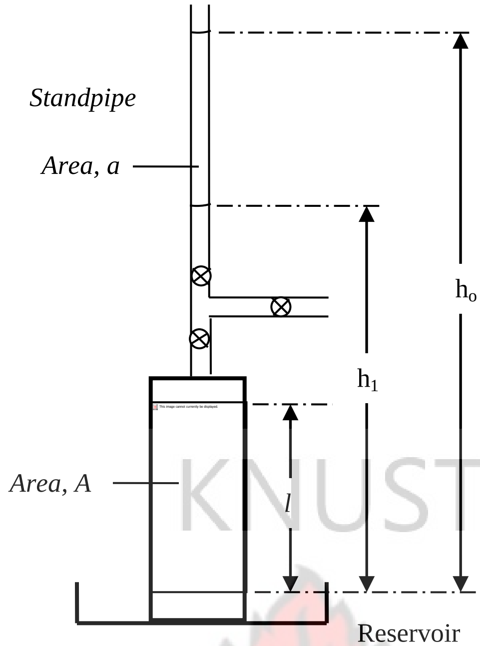

Figure 3.3: Schematic diagram for permeability test

- From Appendix II the test was conducted three times with slightly varying permeability values deduced as follows:

3.5.3 Determination of Soil Porosity

The total porosity of a soil sample is found by knowing the volume of solid material in a given sample of soil and that of the void spaces in the sample. Thus, porosity, n is given by:

(Ya. F. Masalov, 1970) is given by

3.6.1 Discritization of Equations by the Finite Difference Approach

Numerical solutions produce answers at discrete points in the computational domain. These points are called grid points. Grid points show the velocity and pressure storage arrangements within the area under computation.

In the three dimensional space the velocity and pressure configurations show a clearer perspective of the real life situation of the behavior of these fluid flow parameters. However, this present work focuses on two dimensional numerical solution of the mobility of water soluble pollutants in the soil layers.

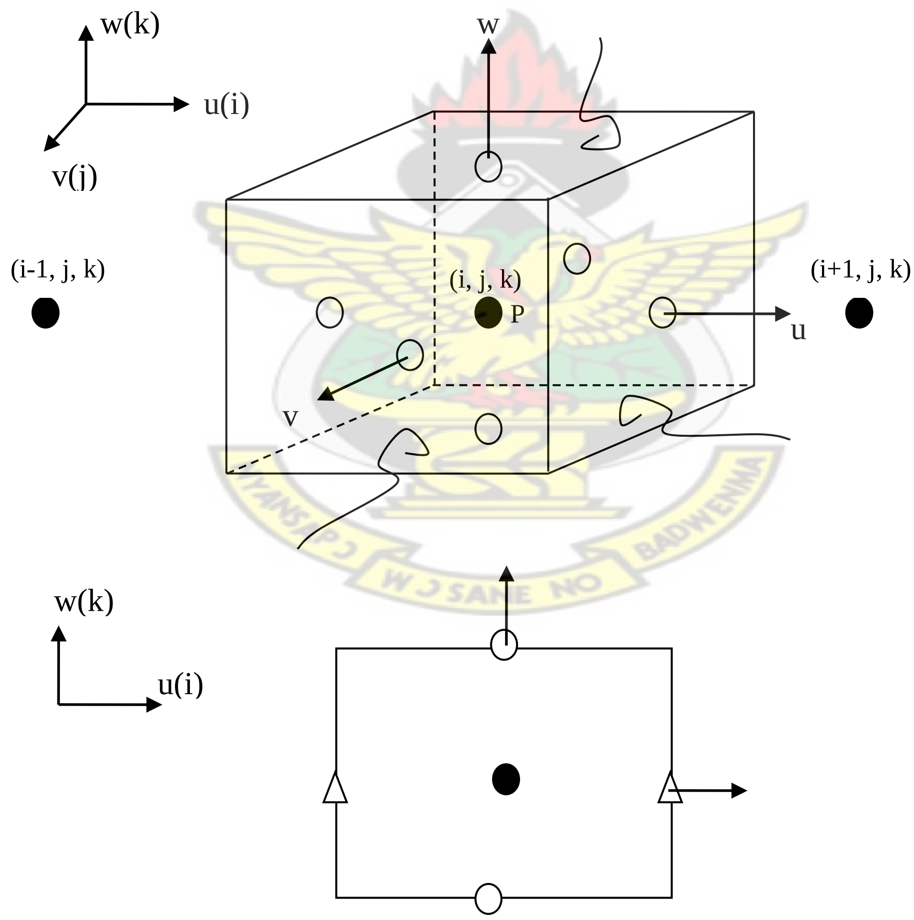

Figure 3.4: Velocity and pressure storage configuration for a staggered grid layout for three and two dimensional space respectively.

Table 3.1: Summary of Difference Equations for some Partial Differential Equations

Differential	Discritization	Type
		Forward difference
		Central difference
		Forward difference

Using the two-dimensional staggered grid below, some basic partial differential equations could be obtained in the difference equations forms as shown in table 3.1 above.

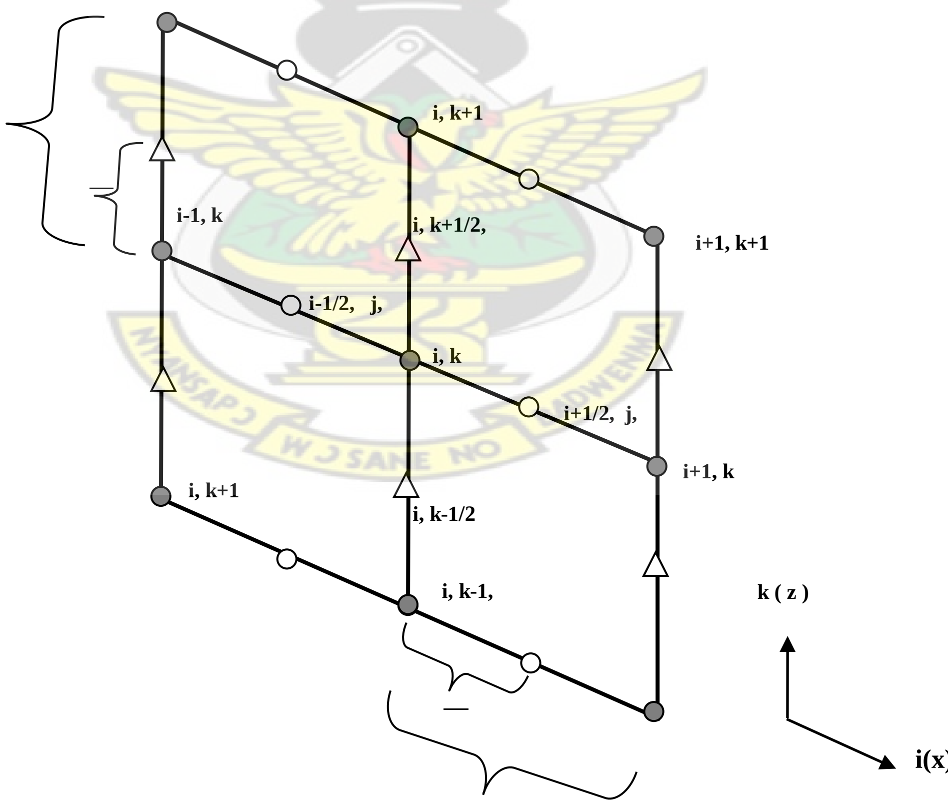

Filled circle pressure p, outline circle u, x-velocity, triangle w, z-velocity component.

Figure 3.5: Two Dimensional Staggered Grids.

A central difference equation representing equation (3.4c), centered around point (i, j) is given by:

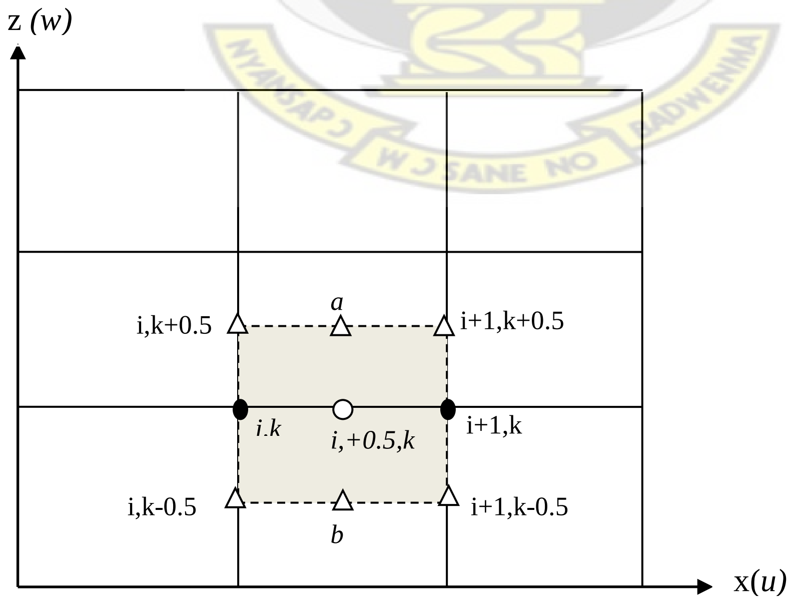
z (w)
a
i,k+0.5
i+1,k+0.5
i.k
i,+0.5,k
i+1,k
i,k-0.5
i+1,k-0.5
b
x(u)

Figure 3.6a: Effective control volume of a computational module to show average velocity in the x-direction

At point *a*:

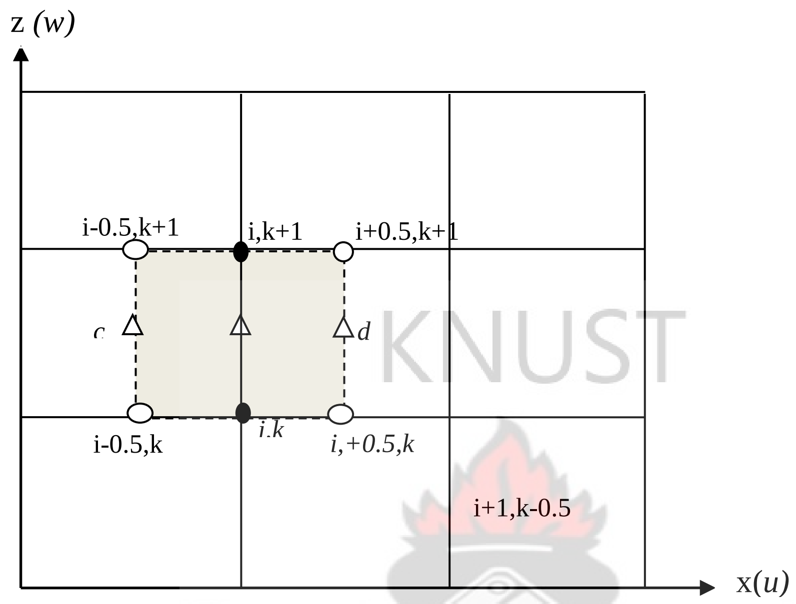

….. (3.15b)

The difference in velocity

3.7.1 The Modified SIMPLE Algorithm for the Numerical Iteration Process

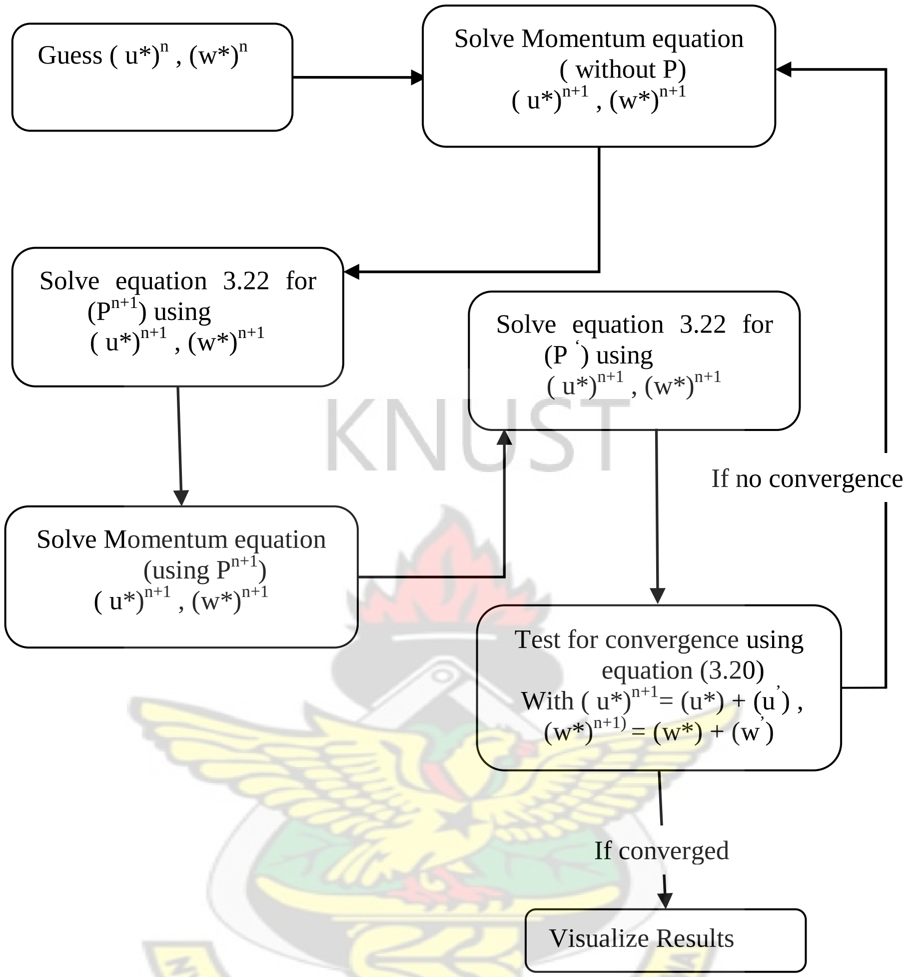

Figure 3.7: Flow chart for Modified SIMPLE Algorithm

3.7.2 Representative Model and Boundary Conditions for Numerical Iteration

Consider a level ground of area 2m x 2m filled with soil to a depth less than 5cm and is supplied with droplets of water soluble pollutant linearly at the Northern boundary. Water would spontaneous flow from the manifold onto the level ground. Once boundary conditions along the model are established it is possible to determine the velocities within the computational domain using iteration methods. The following boundary conditions are observed and assumed:

1. **Inflow Boundary**

At the inflow,

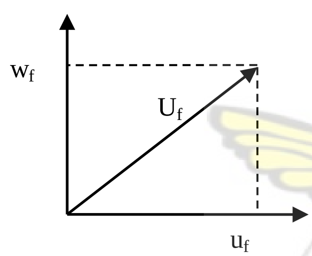

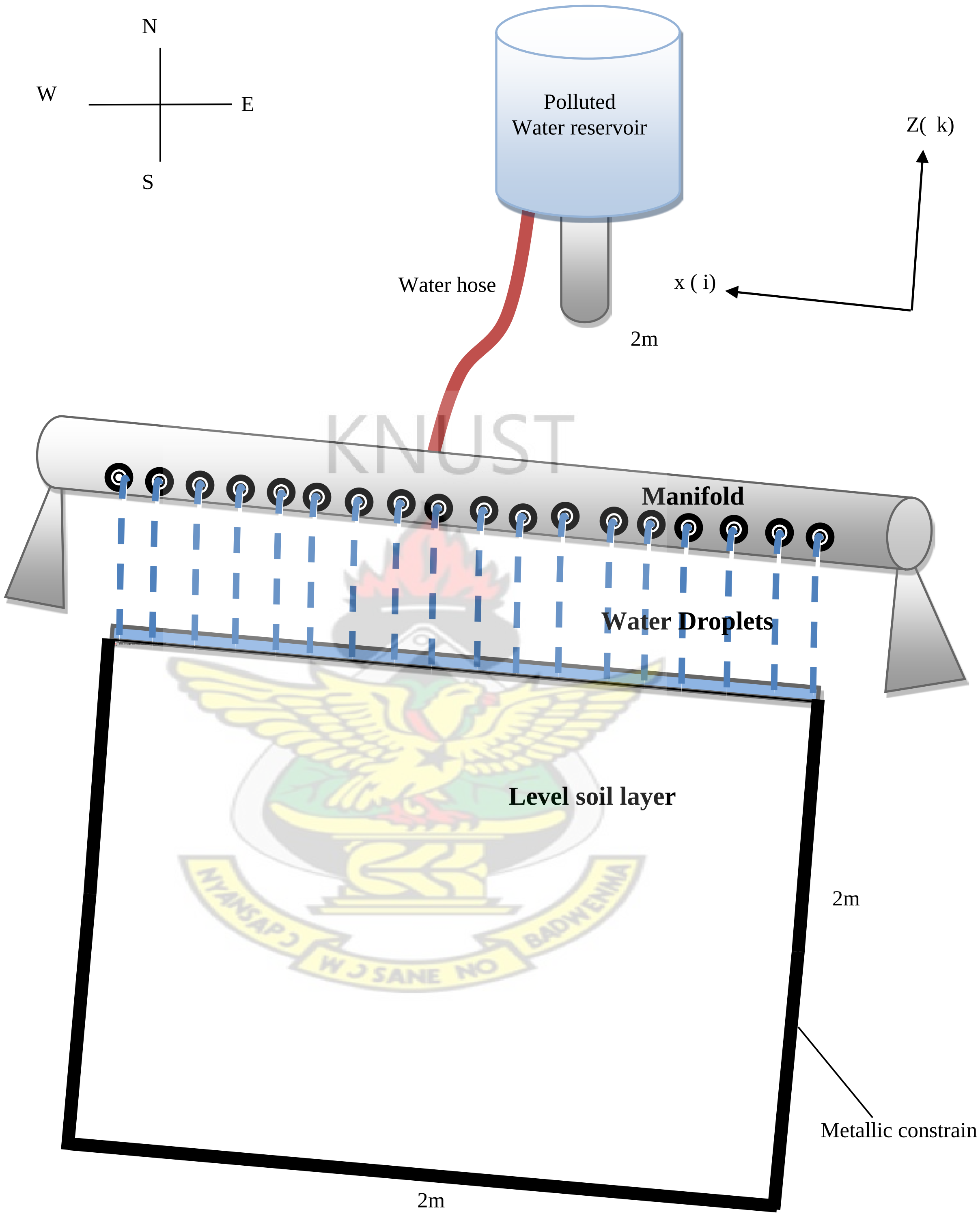

Figure 3.8: Representative Model; Polluted Water at a height flowing into a level Soil layer with metallic constrains.

3.8 Matrix Approach of Solving the System of Equations

The most convenient way of obtaining numerical solutions to real life problems is to model and simulate the problem with computers using the correct and compatible programming language. Experience have shown that MATLAB (Matrix Laboratory) is the best programming language for solving problems involving system of equations that must be iterated periodically before arriving at a close solution. In section 3.7, few points could be iterated using the equations 3.11, 3.12a and 3.12b. However, this is woefully inadequate to predict the flow within the computational domain. Therefore, a more reliable and efficient way of computing the velocities within the computational domain of the same Representative Model above (fig.3.6) is to use the matrix approach which demands that all points within the computational domain are iterated within a certain time step and then visualized for rejection or acceptance.

3.8.1 Spatial Discritization and Transformation of Porous Flow Equations

For the sake of simplicity, let equations 3.12, 3.13a and 3.13b be written using the spatial staggered grid in fig.3.7 below. These equations could be transformed using the table 3.2 below. The simplified transform equations representing equations 3.12, 3.13a and 3.13b are;

Advective = - Pressure - Convective - Constant (Laminar Resistance)

Table 3.2: Spatially Discritized Points and their Transform Notations

Flow Term *(X and Z Components)*		**Discritization**	**Transform Notation**
Advective			
Convective			
Pressure			
Laminar Resistance			
x- continuity component			
Z continuity component			

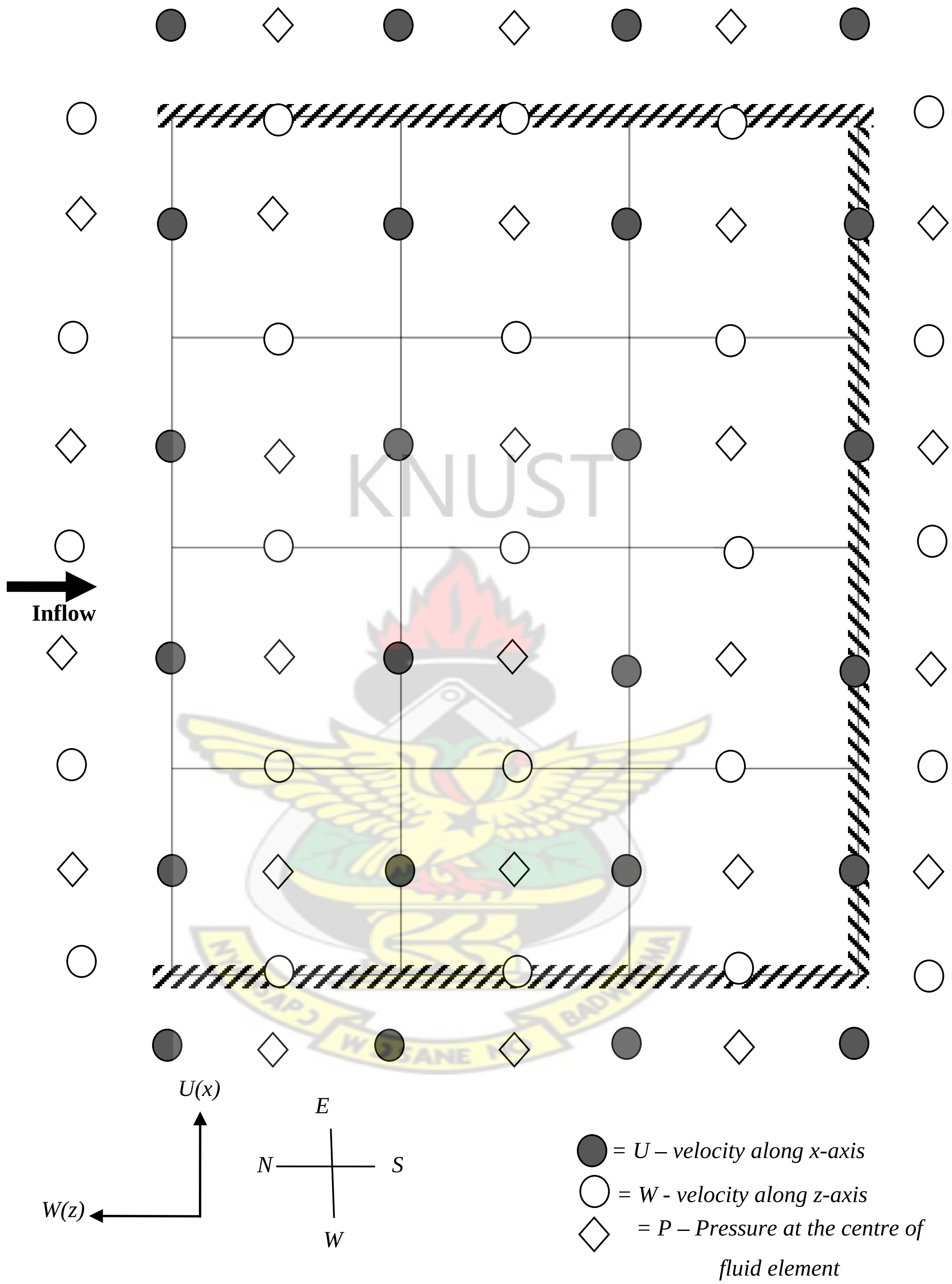

Figure 3.9: Rectangular Spatial staggered grid for a two-dimensional flow

3.8.2 Numerical Solution to the Matrix Approach

Denoting the numerical approximations of the velocities and pressures by capital letters (U, W, and P) and the actual solutions by small letters (u, w and p), gave equations (3.24), (3.25a) and (3.25b) as mentioned above. Assuming that there is a set of velocities in the velocity fields $\mathbf{U}^{\mathbf{n}}$ and $\mathbf{W}^{\mathbf{n}}$ at the nth time step (t) and ensuring that equation (3.24) is not violated. The various terms in the equations are manipulated for an approximate solution as follows:

Convective Term

The convective terms are non-linear but could be solved by circumventing explicitly to arrive at the solution of the non-linear system of velocities.

Equations (3.24a) and (3.24b) may be rewritten in the vector notation as

3.9.1 Mobility and Concentration of Pollutants in the Computational Domain

The concentration of pollutants could be computed once the velocity fields have been determined. The equation for the mobility of heavy metals in a porous medium like soil is given by

3.10 Flow Chart for the Simulation of Water Soluble Pollutant through Soil Using the Matrix Iteration Method

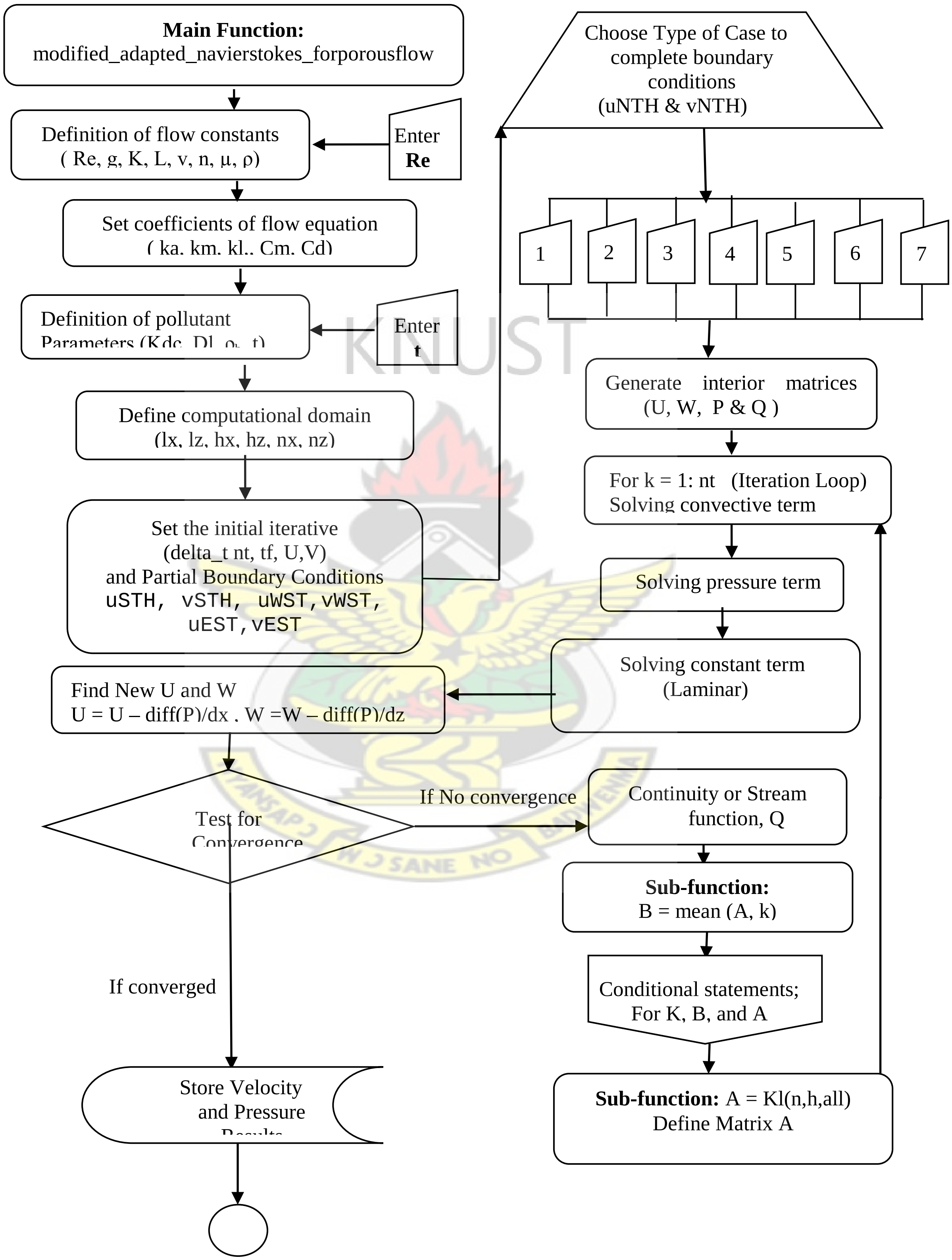

Cont;

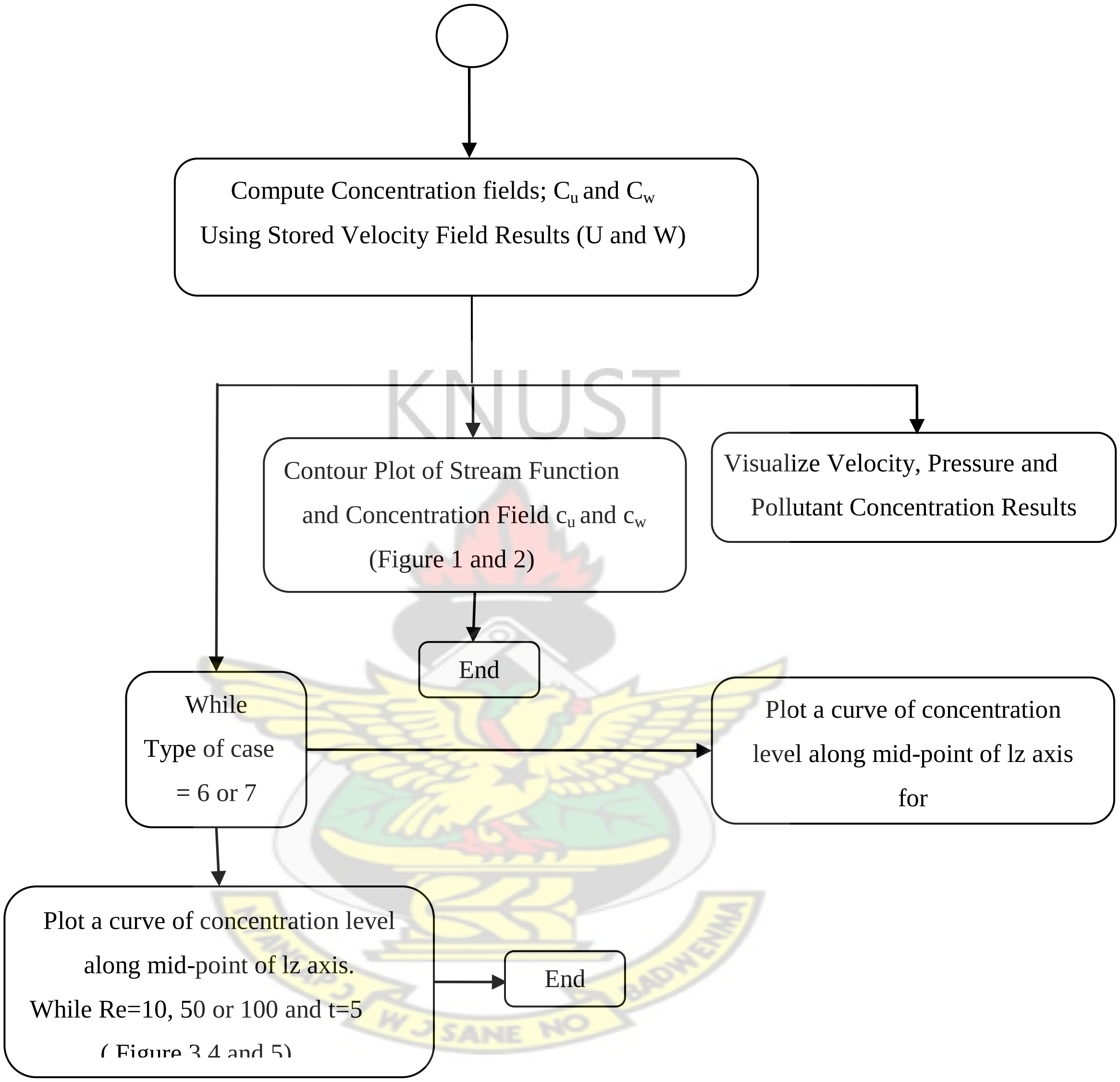

Figure 3.10: Flow chart for modified_adapted_navierstokes_forporousflow

3.11 MATLAB Code for the Simulation of Water Soluble Pollutant through Soil

A code called modified_adapted_navierstokes_forporousflow (Appendix I) has been written and it is used to simulate water soluble pollutant through fine sand. The whole code is a single Matlab file of about 340 lines and it has the following features:

1. It is flexible as far as flow properties and porous media are concern.
2. It is fast in computation for small to moderate mesh size and it produces multiple plots including some subplots.
3. It could be modified to suit and solve three dimensional problems.
4. It is quite versatile as it could solve seven different cases by changing pollutant sources using numeric system of 1 to 7.
5. It could solve for all the different cases using a range of Reynolds numbers from 1 to 2300 (laminar flow regime).
6. Pollutant dispersion times (hrs) could also be easily changed using numbers.

3.12 Experimental Models

Computer results are sometimes deceptive and care must be taken anytime results are obtained from the computer. Hence, the need to build a miniature model that would substantiate results obtained. Figure 3.11 below is a model constructed and used to validate cases 3, 6 and 7. The model comprises;

1. A 2m square wooden wall (boundary) labeled as Northern boundary (Top), Southern boundary (Bottom), Eastern boundary (Right) and Western boundary (left).

2. A water proof rubber carpet beneath the 2-m square wooden wall.
3. 3-cm depth of fine sand (plastering sand) evenly and horizontally spread on the carpet within the square wall.
4. Eight hooking pegs that firmly hold the wooden walls on to the level ground.
5. 2-m long, 1 inch diameter PVC pipe with linear perforations and both ends closed.
6. Water hose fixed with epoxy glue that connects the reservoir to the PVC pipe.
7. Reservoir containing dye solution.
8. Reservoir stand
9. A pair of PVC pipe stands.

Figure 3.11: Experimental model for validation of simulated results

3.12.1 Assumptions

The following assumptions are made:

1. The thickness of fine sand with the 2-m square wooden wall is assumed to be of unit depth. This condition is necessary when dealing with 2D flow through the fine sand.
2. The square wooden wall is assumed to water proof.
3. The carpet and wooden boundary should not undergo any form of chemical reaction.
4. The natural orientation of the sand particles s well as its associated porosity and permeability is assumed to be unchanged.
5. The flow of dye from the PVC pipe through the perforations is assumed to be of equal and uniform flow rate (drop rate).
6. The pressure with which the dye enters the sand is assumed to be equal to atmospheric pressure.
7. Concurrently, the flow of the dye through the sand is assumed to be purely laminar flow throughout with a lower Reynolds number.

CHAPTER 4

RESULTS AND DISCUSSION

4.1 Introduction

The single Matlab file is used to simulate the flow of water soluble pollutant through fine sand. Seven different pollutant source locations (cases) were examined using the same single nested code. Various contour plots and curves which depict the nature of pollutant dispersion and level of its concentration distribution as well as other flow variables such as stream function and pollutant velocity and pressure were obtained. Simultaneously, two different Reynolds numbers and time intervals were also compared using cases 6 and 7. The results obtained are shown in Figures 4.1 through to Figure 4.24. Another vital aspect of this chapter is the experimental set-up built and used to certify and validate some of the results obtained.

A critical and careful observation and examination of each of the seven different cases considered under section 4.2 reveal and portray similar geometric simulation of pollutant dispersion from a concentrated source. From Figure 4.1 through to Figure 4.10 equal volume and concentration of water soluble pollutants were placed at various positions along the inflow boundary with a coverage area of approximately 10% of the inflow boundary. For Figure 4.11 and 4.12, the same volume and concentration of water soluble pollutant was fully placed along the inflow boundary. Whilst in Figure 4.13 and 4.14, the same volume and concentration of the pollutant was placed at 50% lengthwise by 20% breath within the computational domain and all the four boundaries fixed. For each of Figures 4.1 to 4.14, figures that show single graphs are composite plots whilst those containing a set of plots give subplots for individual flow variables.

4.2 Contour and Streamline Plots for Pollutant Distribution and Flow variables

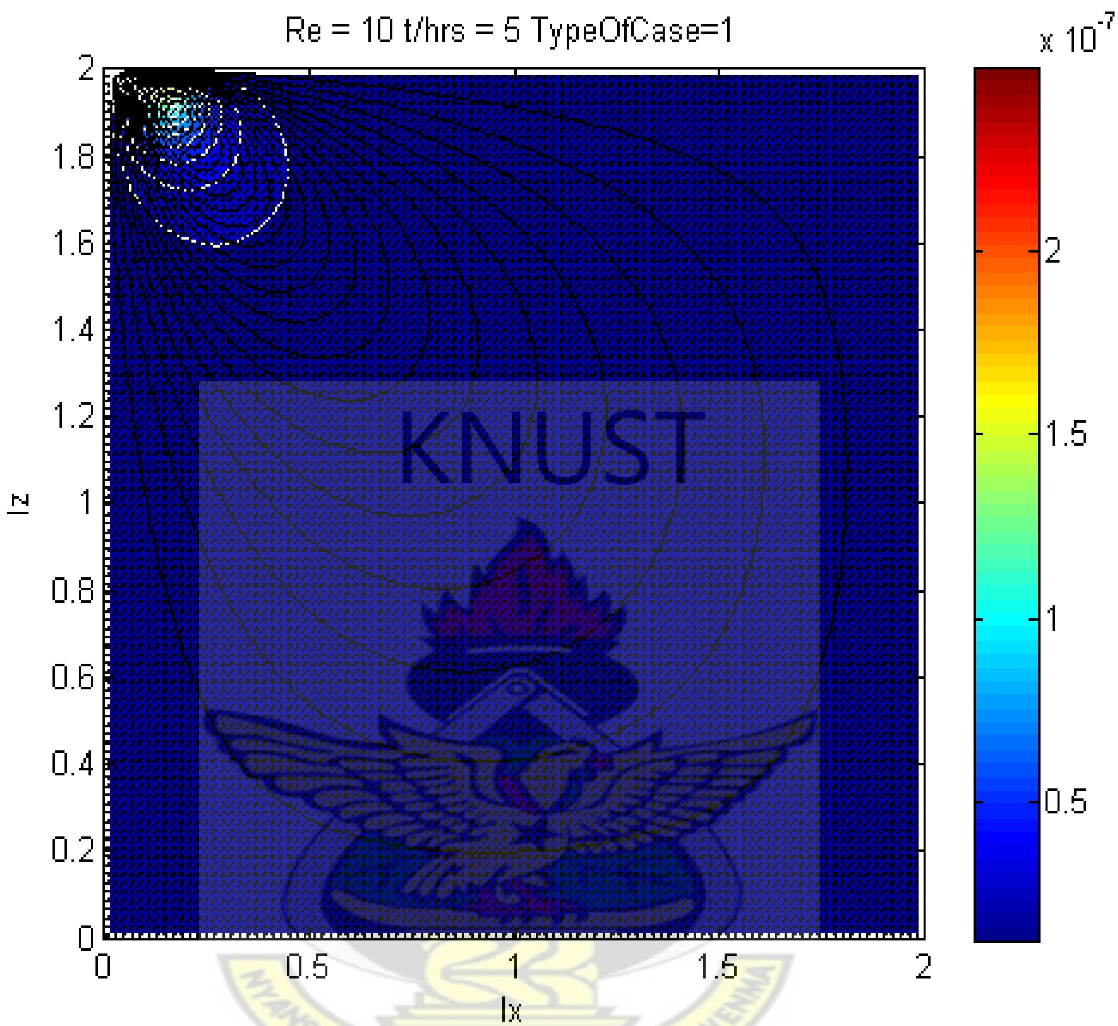

(Case 1: Water soluble pollutants placed at the inflow (North) to cover 10% of the Northern boundary length just after Western boundary)

Figure 4.1: 2D contour and streamline plot for concentration distribution and dispersion of a water soluble pollutant through fine sand for case 1.

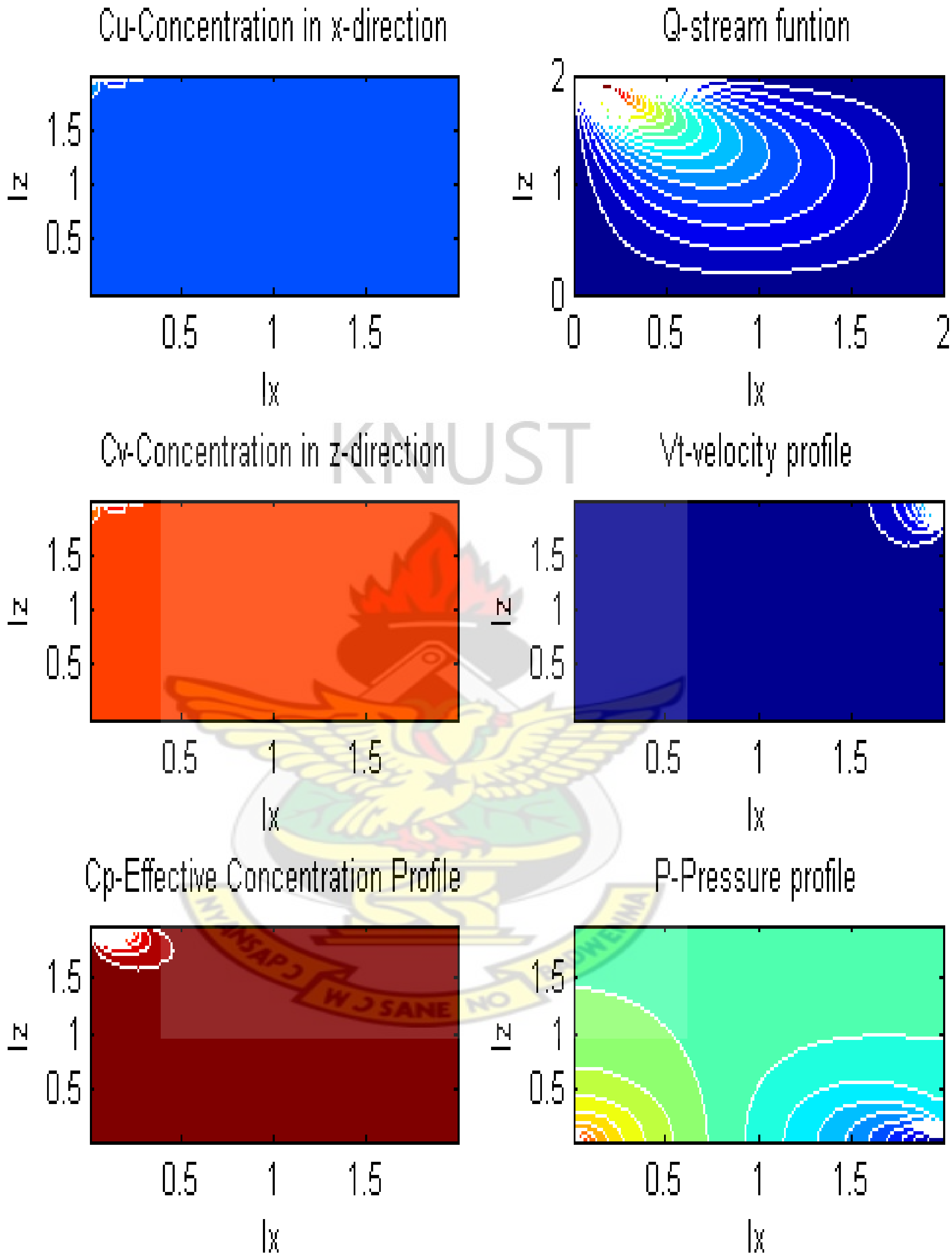

Figure. 4.2: 2D Contour plots for case 1 flow variables

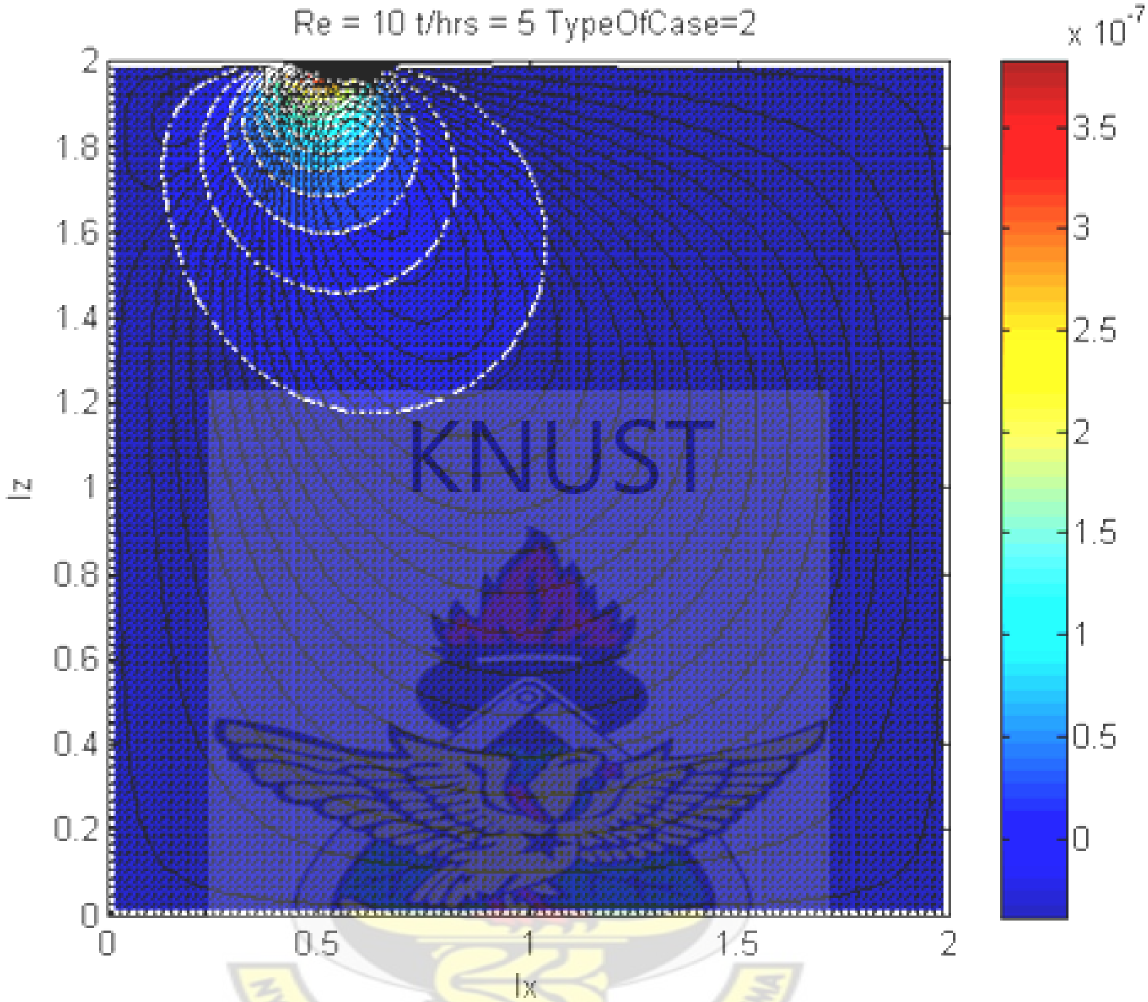

(Case 2: 10% of water soluble pollutant coverage at the inflow in between 20% and 70% of the Northern boundary length from Western to Eastern boundary respectively)

Figure. 4.3: 2D contour and streamline plot for concentration distribution and dispersion of a water soluble pollutant through fine sand for case 2.

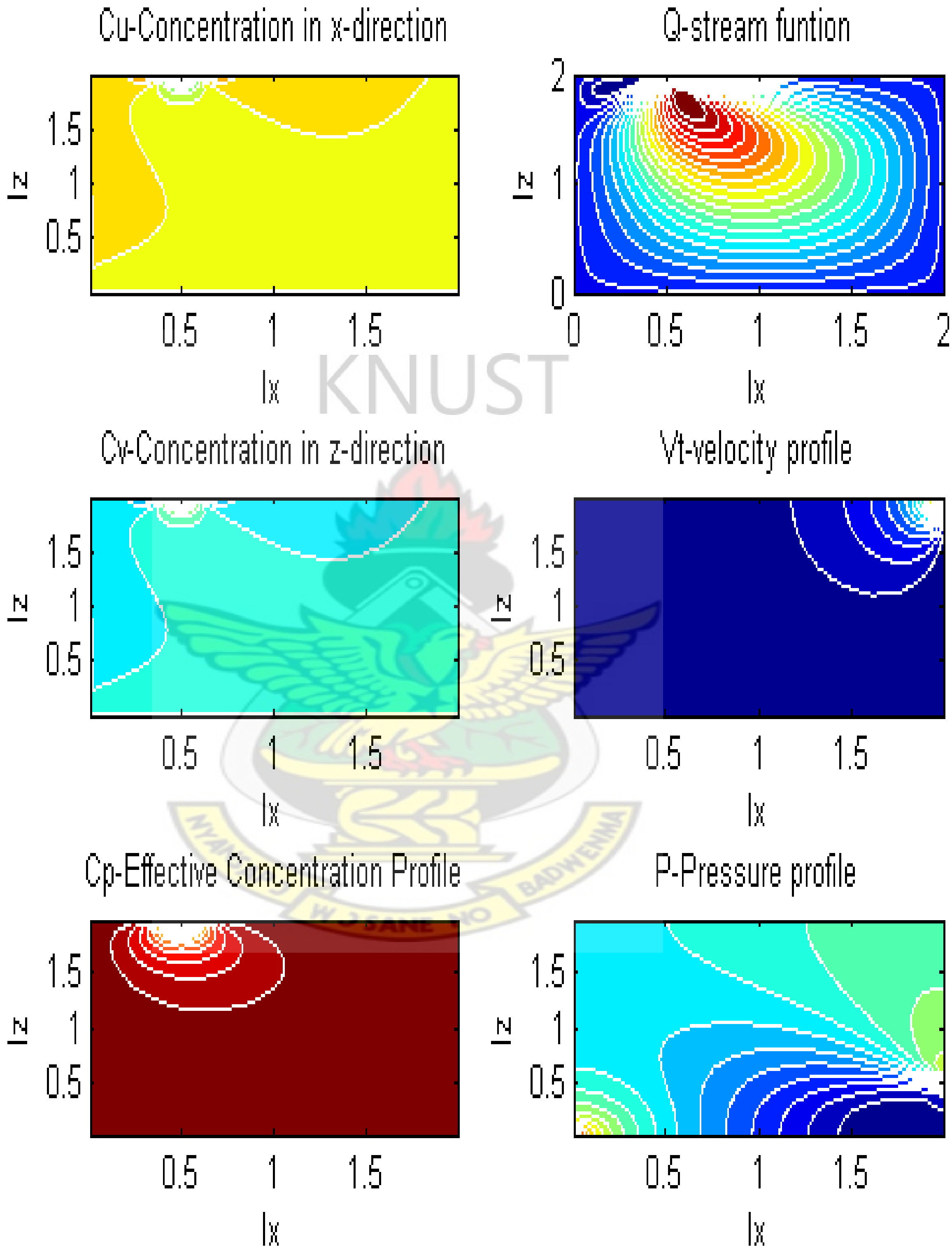

Figure.4.4: 2D Contour plots for case 2 flow variables

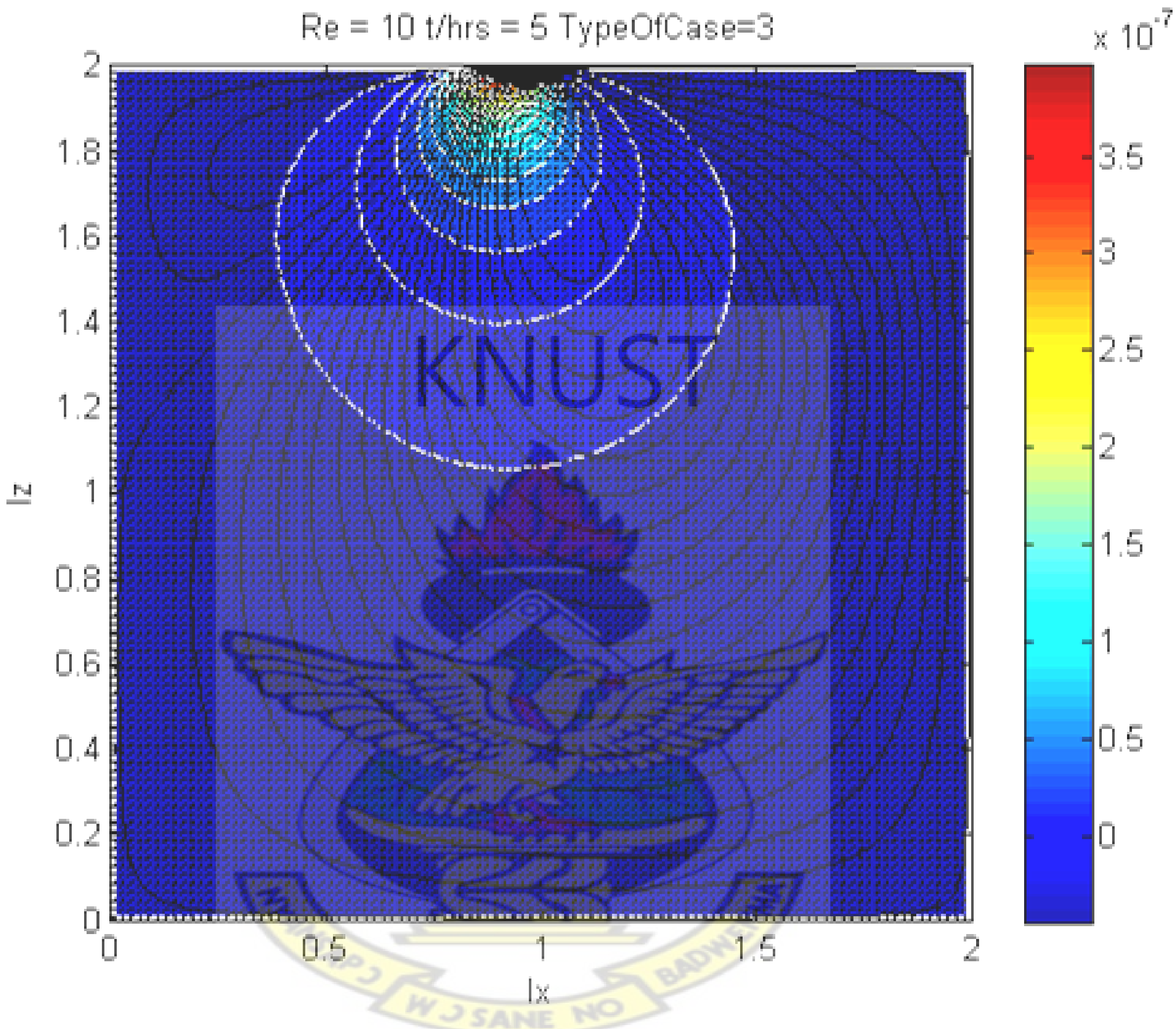

(Case 3: 10% of water soluble pollutant coverage at the inflow in between 40% and 50% of the Northern boundary length from Western to Eastern boundaries respectively)

Figure. 4.5: 2D contour and streamline plot for concentration distribution and dispersion of a water soluble pollutant through fine sand for case 3

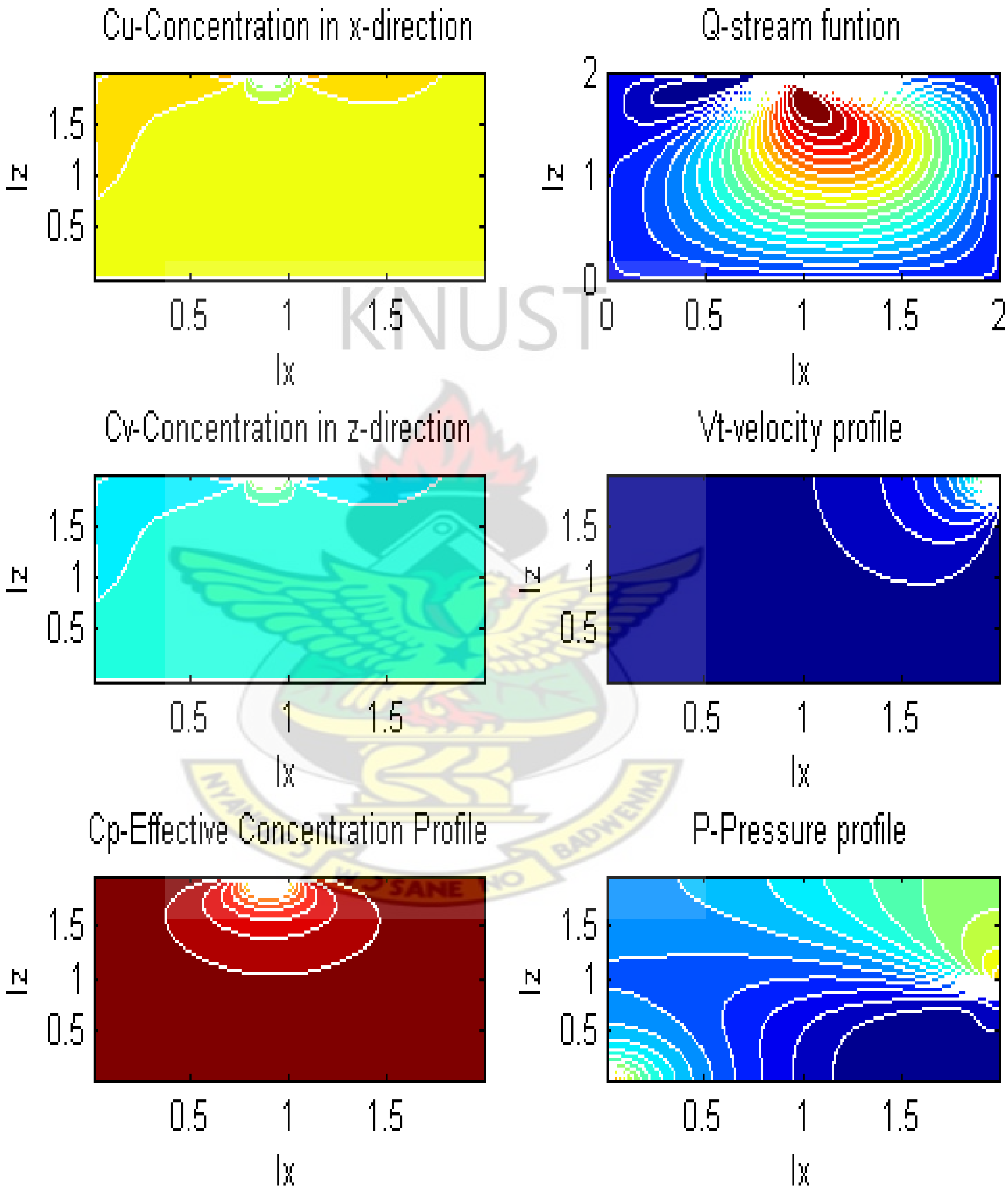

Figure 4.6: 2D Contour plots for case 3 flow variables

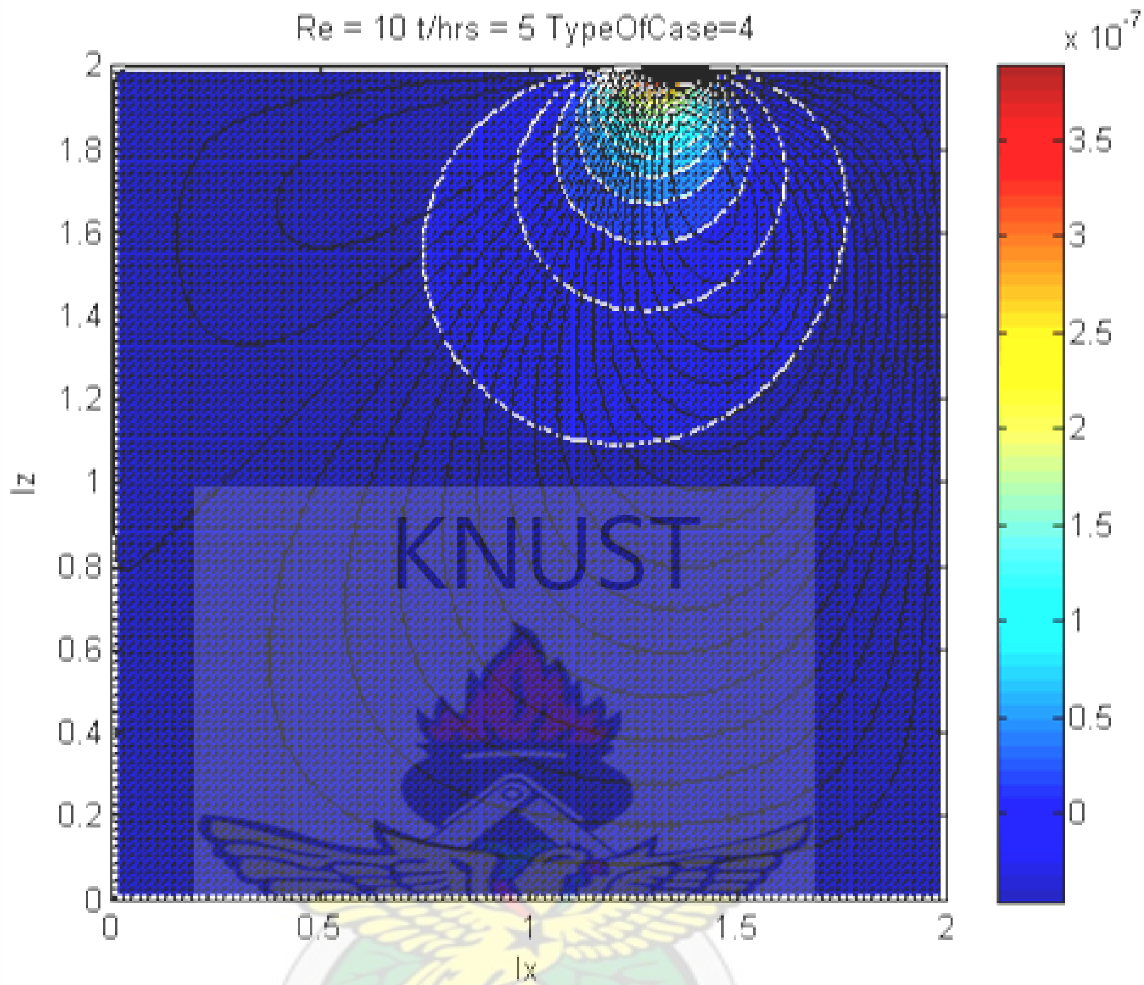

(Case 4: 10% of water pollutants coverage at the inflow in between 60% and 30% of the Northern boundary length from Western to Eastern boundaries respectively)

Figure 4.7: 2D contour and streamline plot for concentration distribution and dispersion of a water soluble pollutant through fine sand for case 4

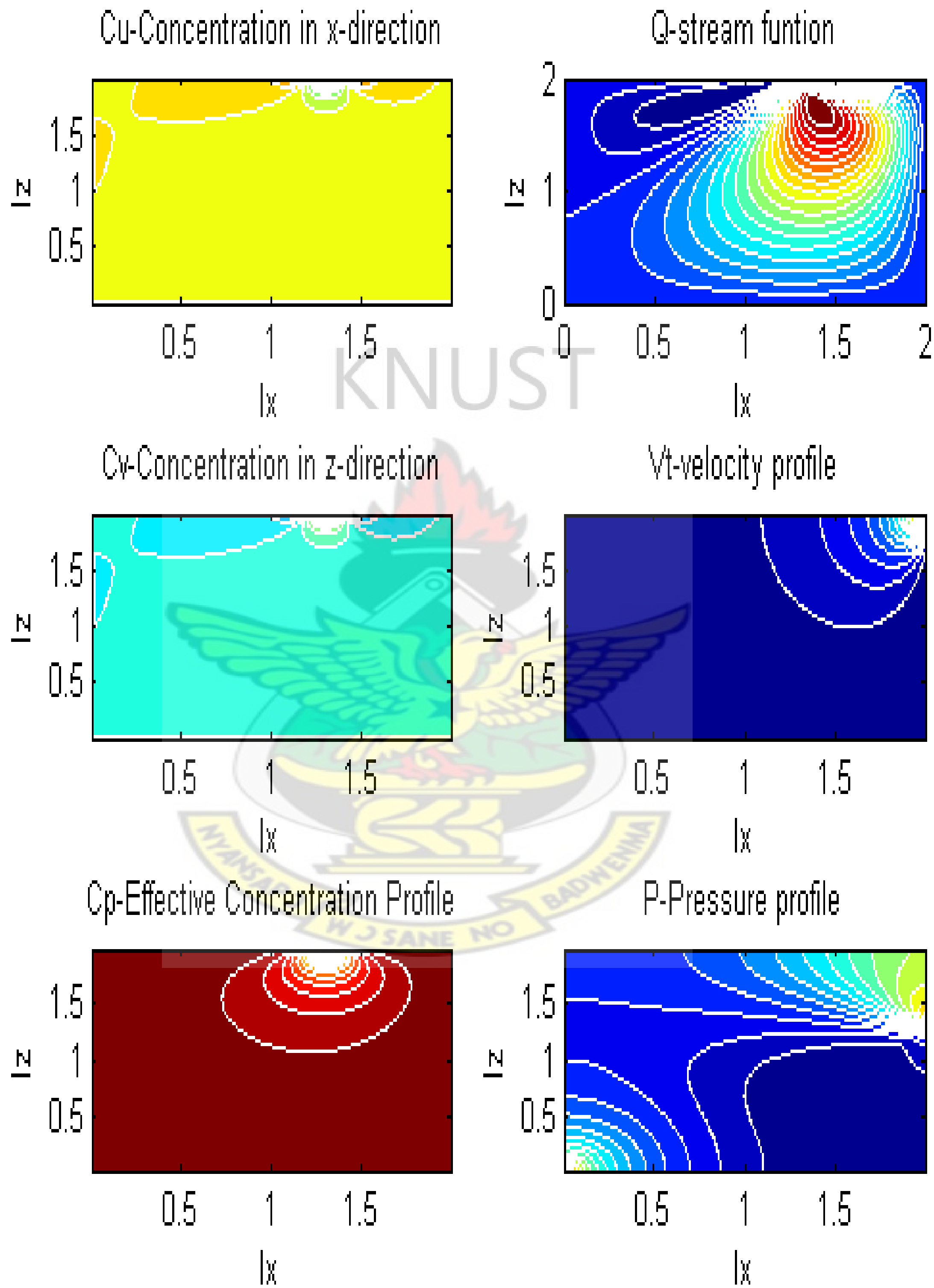

Cu-Concentration in x-direction
Q-stream funtion
Cv-Concentration in z-direction
Vt-velocity profile
Cp-Effective Concentration Profile
P-Pressure profile
lz
lx
0.5
1
1.5
0
2

Figure 4.8: 2D Contour plots for case 4 flow variables

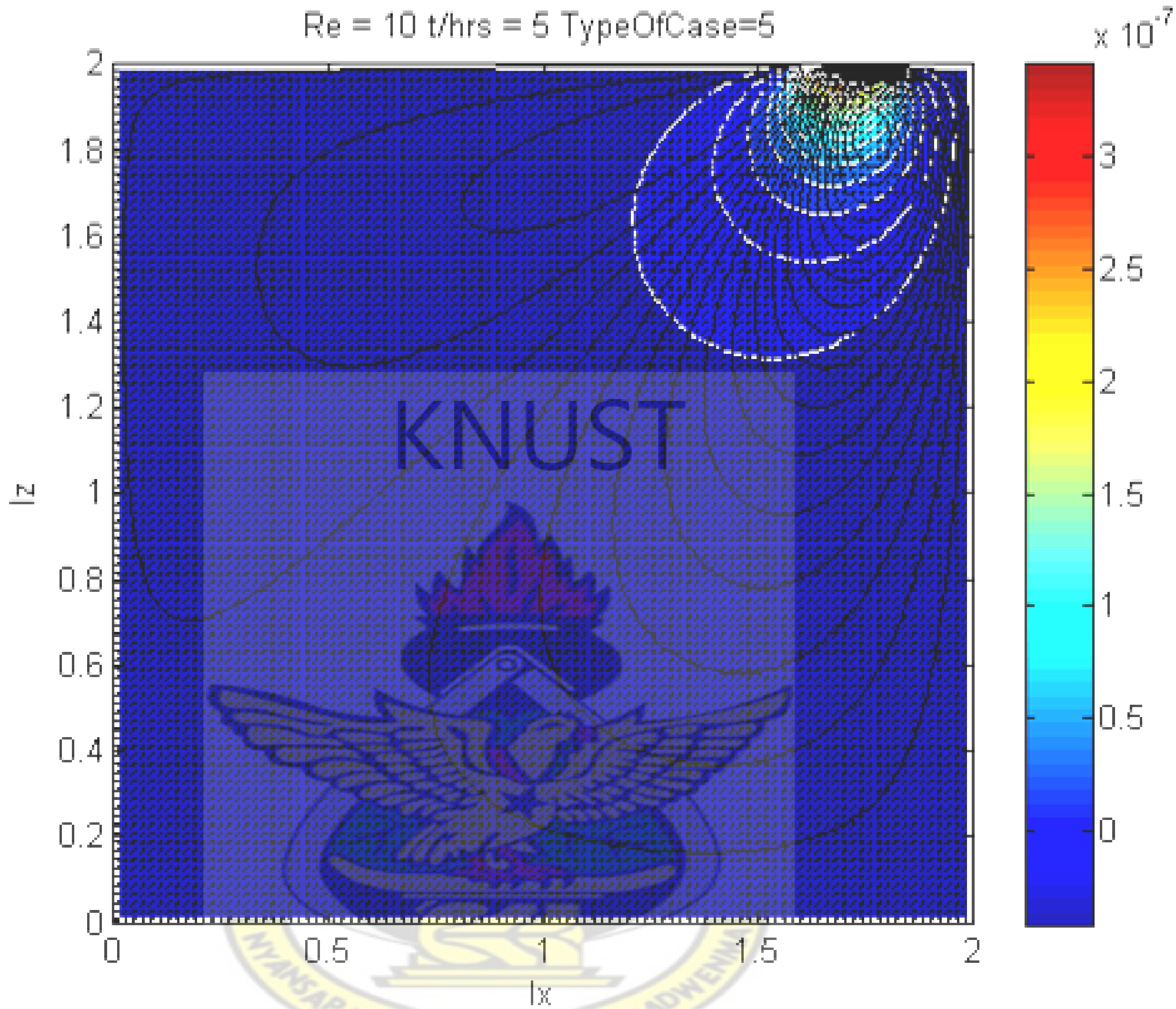

(Case 5: 10% of water pollutants coverage at the inflow in between 80% and 10% of the Northern boundary length from Western to Eastern boundaries respectively)

Figure 4.9: 2D contour and streamline plot for concentration distribution and dispersion of a water soluble pollutant through fine sand for case 5.

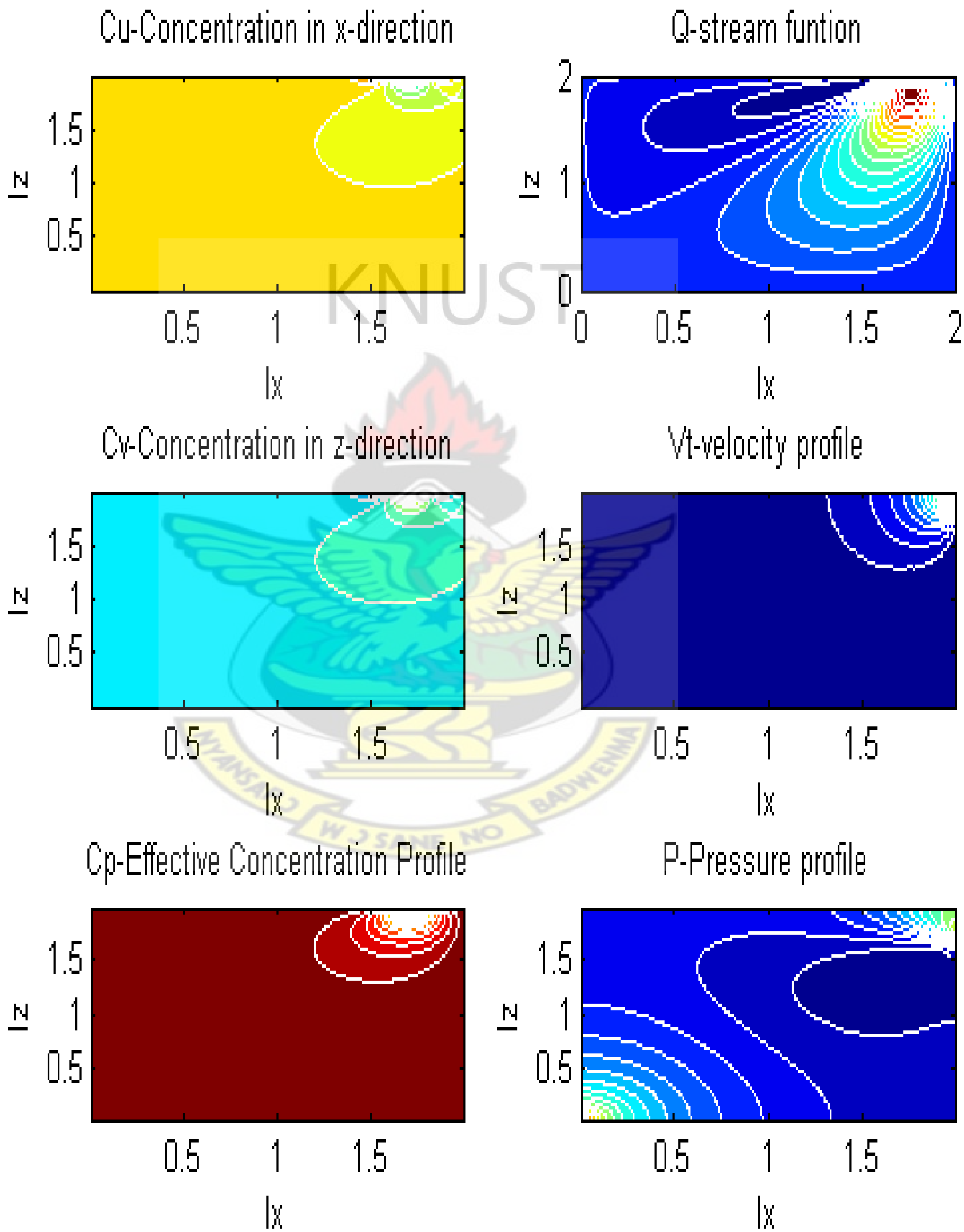
Cu-Concentration in x-direction
Q-stream funtion
Cv-Concentration in z-direction
Vt-velocity profile
Cp-Effective Concentration Profile
P-Pressure profile
lz
lx
0
0.5
1
1.5
2

Figure 4.10: 2D Contour plots for case 5 flow variables

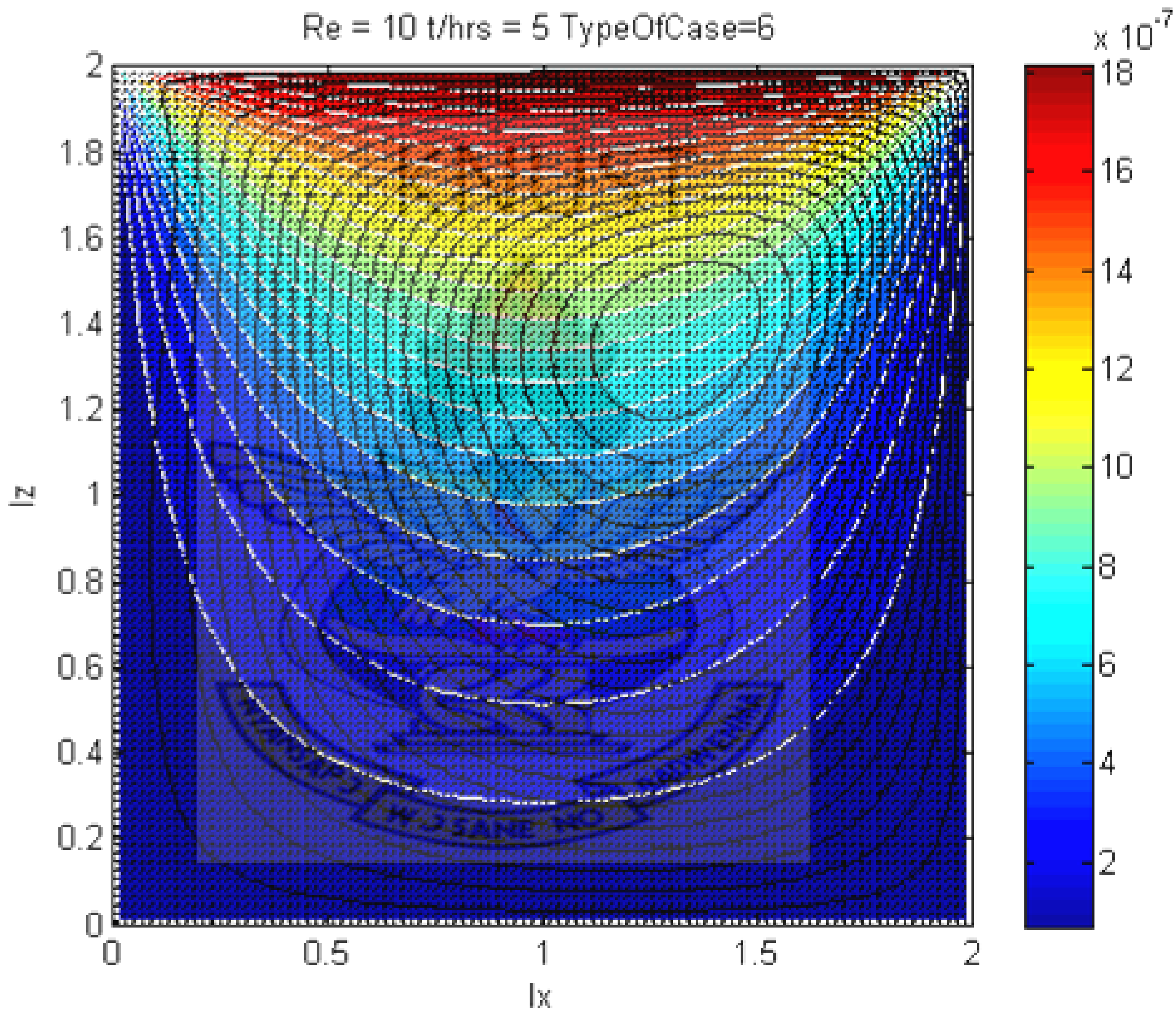

(Case 6: 100% of water soluble pollutant coverage at the inflow along the Northern boundary)

Figure 4.11: 2D contour and streamline plot for concentration distribution and dispersion of a water soluble pollutant through fine sand for case 6

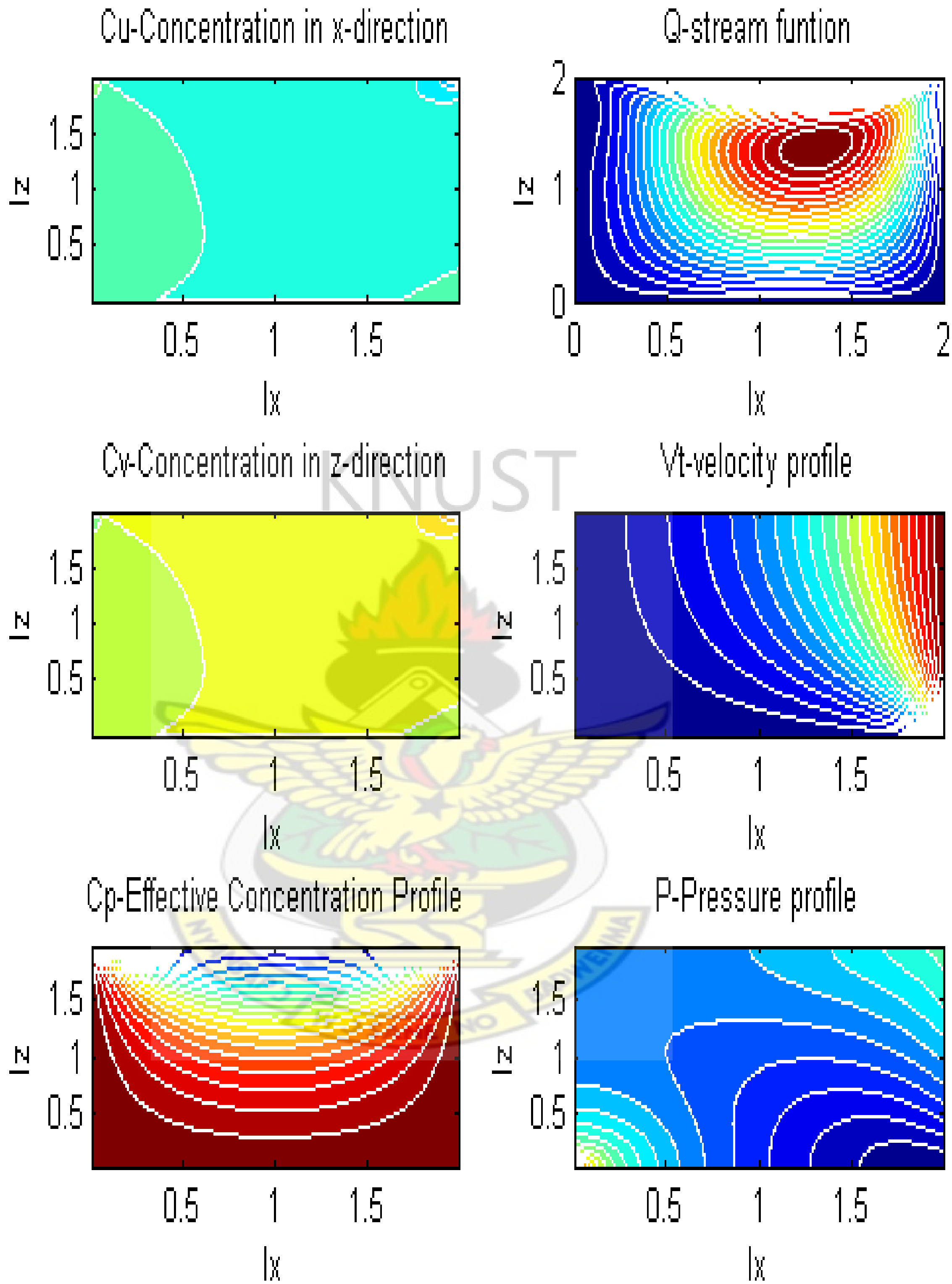

Figure 4.12: 2D Contour plots for case 6 flow variables

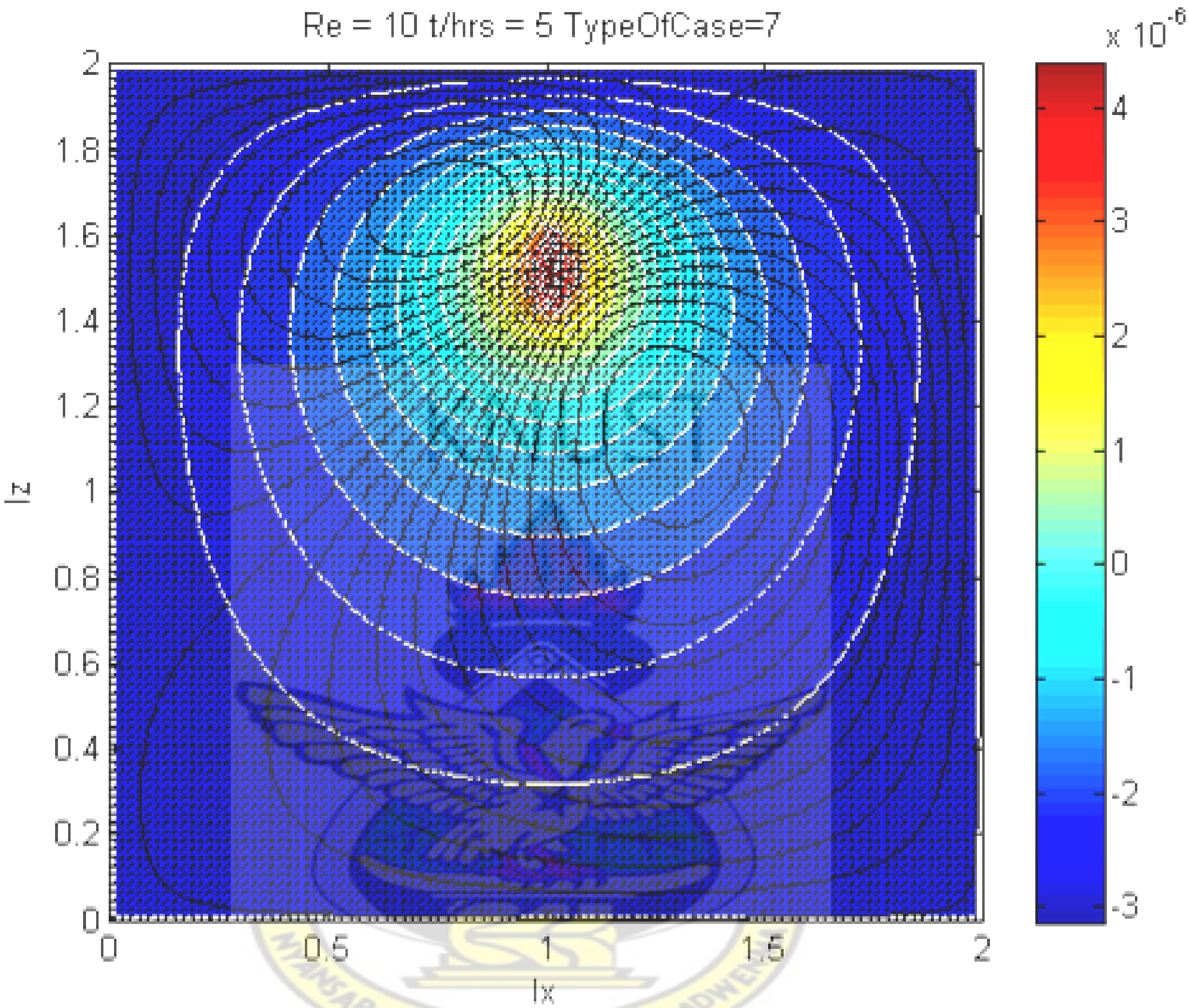

(Case7: 10% of water soluble pollutant coverage at 50% lengthwise by 20% breadth within the computational domain with fixed boundaries at North, South, East and West)

Figure 4.13: 2D contour and streamline plot for concentration distribution and dispersion of a water soluble pollutant through fine sand for case 7

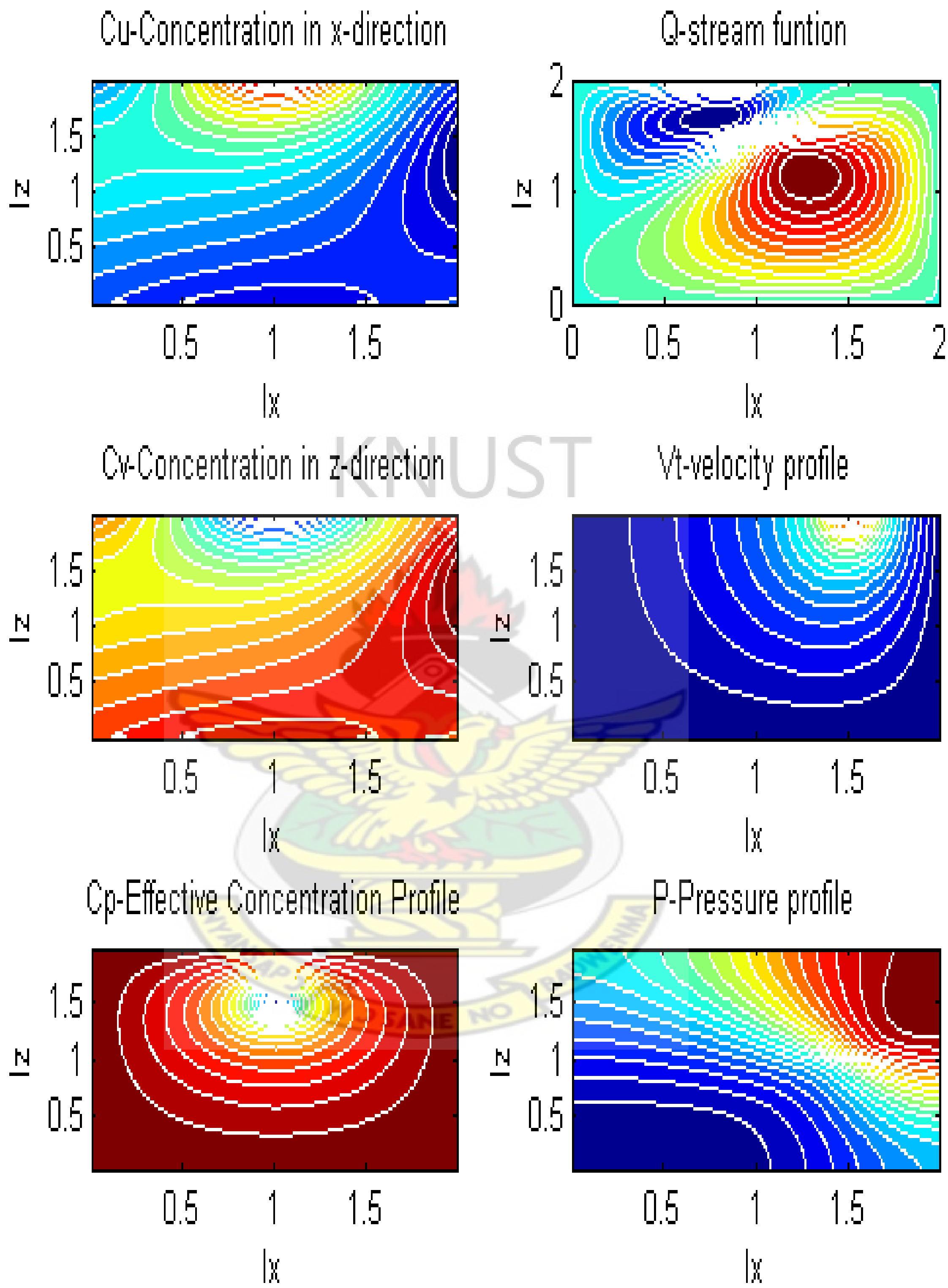

Figure 4.14: 2D Contour plots for case 7 flow variables

4.3 Interpretation of Contour Plots

In Figure 4.1, the pollutant was placed along the Northern boundary (inflow) just after the Western boundary. It could be observed that the pollutant dispersed in a conical wave form as it mimics the behavior of the stream function. A closer look at the colour bar gives a vivid indication of the fact that the magnitude of the concentration decreases from the source with a pink colour to the sink with a blue colour. Its corresponding flow variables from Figure 4.2 also follow suit. Thus the Cu-concentration, Cv-concentration and the Cp-effective concentration plot as well as the stream function follow similar pattern. This is true because the concentration distribution in all of these sub-cases died out gently form the source whilst spreading uniformly in a conical manner to the sink within the computational domain.

Another model was simulated by placing the pollutant source in between 20% and 70% length wise along the Northern boundary from the Western and Eastern boundaries respectively such that the pollutant source occupies approximately 10% of the boundary length. It is clear from Figure 4.3 that the water soluble pollutant dispersed in a crooked eccentric manner as the concentration from the source to the sink declined gently. Concurrently, nearly all of the flow variables such as stream function and effective concentration in Figure 4.4 also spread in an eccentric wave form.

It is very interesting to visualize that as the pollutant source was further moved along the Northern boundary at about 40% lengthwise way from the Western boundary, a true eccentric wave form dispersion of the pollutant was obtained. This is evident from Figures 4.5 and 4.6 as the flow pattern resembles that obtained in Figures 4.3 and 4.4.

Again, the pollutant level was moved to different a position at approximately 60% lengthwise along the Northern boundary away from the Western boundary. This time, the pollutant dispersed in a less crooked eccentric pattern similar to that obtained in case 2 (Figures 4.3 and 4.4). Figures 4.7 and 4.8 give the geometry of the pollutant distribution pattern as it confirms the true similarity and linkage between case 4 and case2.

Finally, when the pollutant was placed in between 80% and 10% lengthwise along the Northern boundary from Western and Eastern boundaries respectively, the pollutant dispersion pattern deviated slightly from that experienced in case 1(where pollutant was placed just beside the fixed Western boundary). However, there exist a very close correlation between this case and case 1 as conical wave form dispersion of the pollutant from the source to sink was achieved (Figure 4.9 and 4.10). The geometric suspicion and in fact the true picture is that in both cases the pollutants were placed close to the fixed boundaries (Western and Eastern boundaries respectively).

Moreover, a unique situation was also considered where the entire pollutant was placed along the whole length of the Northern boundary. From Figure 4.11 and 4.12, it could be visualized that the pollutant dispersed in a U-shaped wave form as the concentration levels fall gently from the source to the sink. Here too the flow variables such as velocity profile, stream function as well as effective concentration distribution all follow suit.

A more unique development was considered where the pollutant was placed within the computational domain 50% lengthwise by 20% breadth. This is illustrated in Figures 4.13 and 4.14. As clearly observed, a true concentric wave form dispersion of the pollutant is exhibited. The concentration of the pollutant once again, decreases from the source (with pink colour) to the sink (with blue colour) as indicated by the colour bar.

4.4 The Influence of Reynolds Number on Pollutant Distribution

The concentration levels along the mid-point of lz (breath of the computational domain in the z-direction) at various Reynolds numbers within the laminar flow regime for a five hour interval were simulated and compared. Reynolds numbers 10, 50 and 100 were used for the simulation by plotting the concentration levels along the mid-point of lz against lx (nx) (the length of computational domain along x-direction) for cases 6 and 7. The following graphs (Figure 4.15 through to Figure 4.18) shows the results obtained for cases 6 and 7.

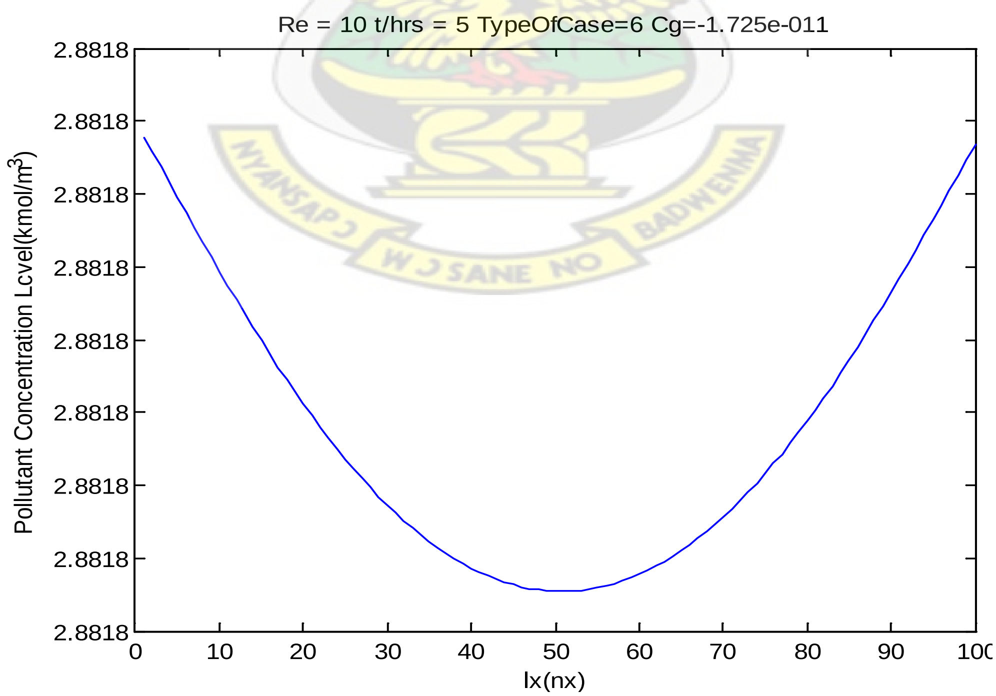

Figure 4.15: Concentration Profile along the Mid-point of lz-axis for case 6 with Re=10

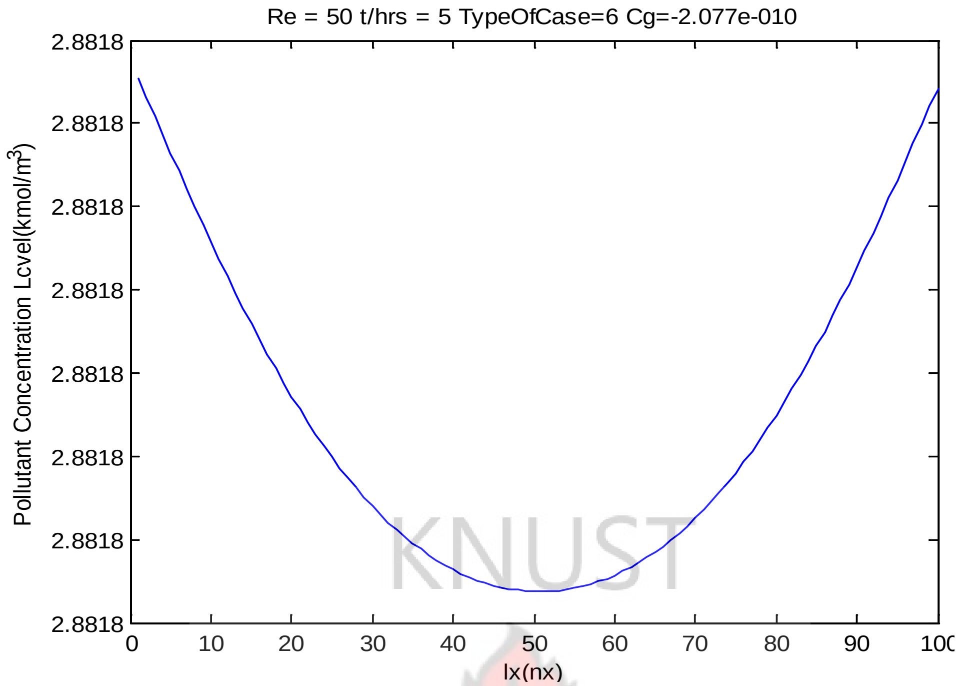

(a)

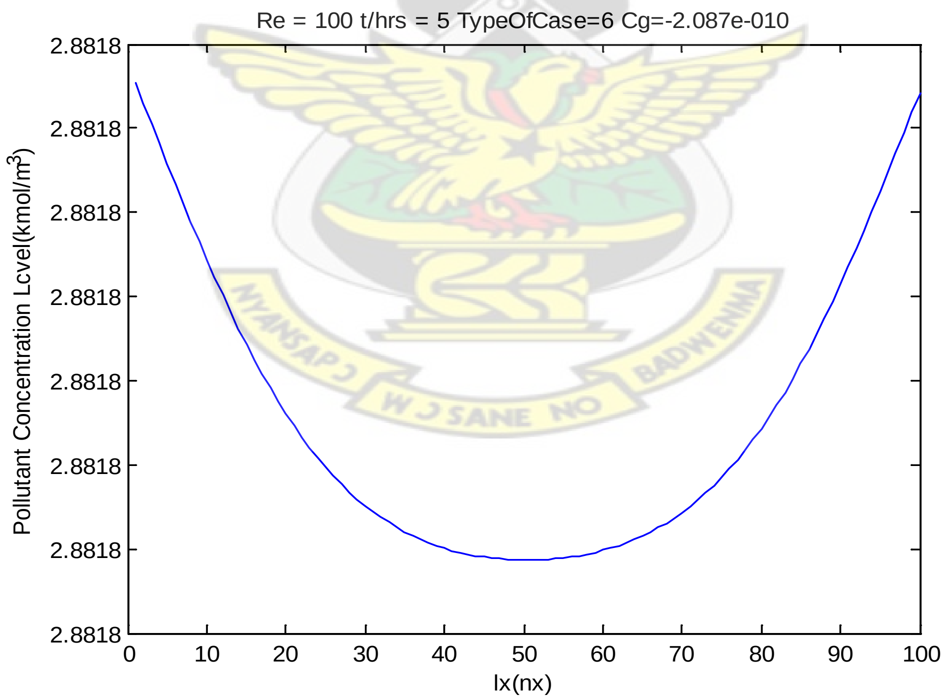

(b)

Figure 4.16: Concentration Profile along the Mid-point of lz-axis for case 6 with;

(a) Re=50 and (b) Re=100.

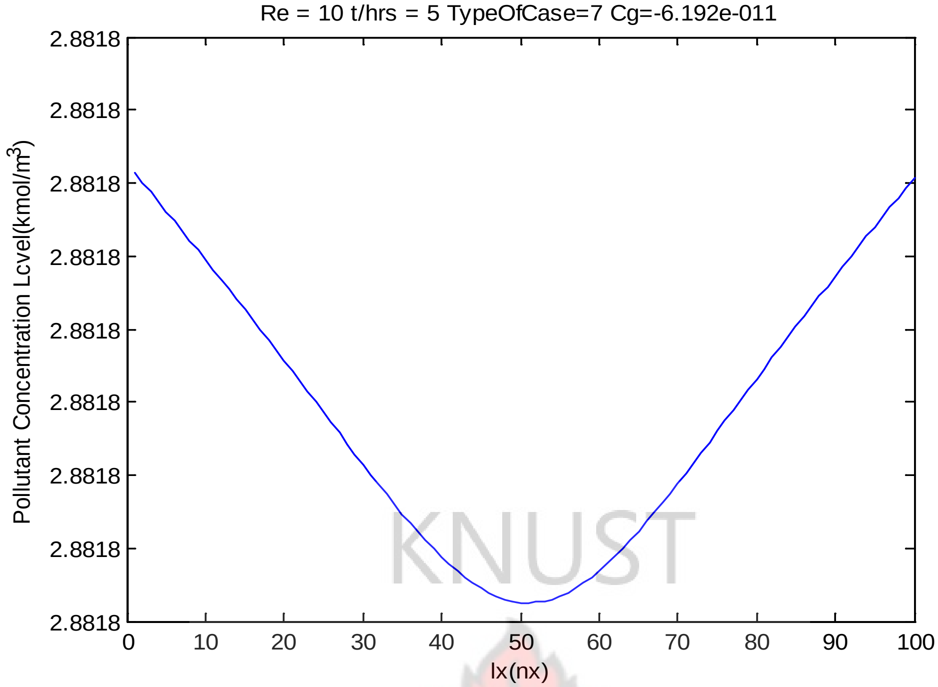

(a)

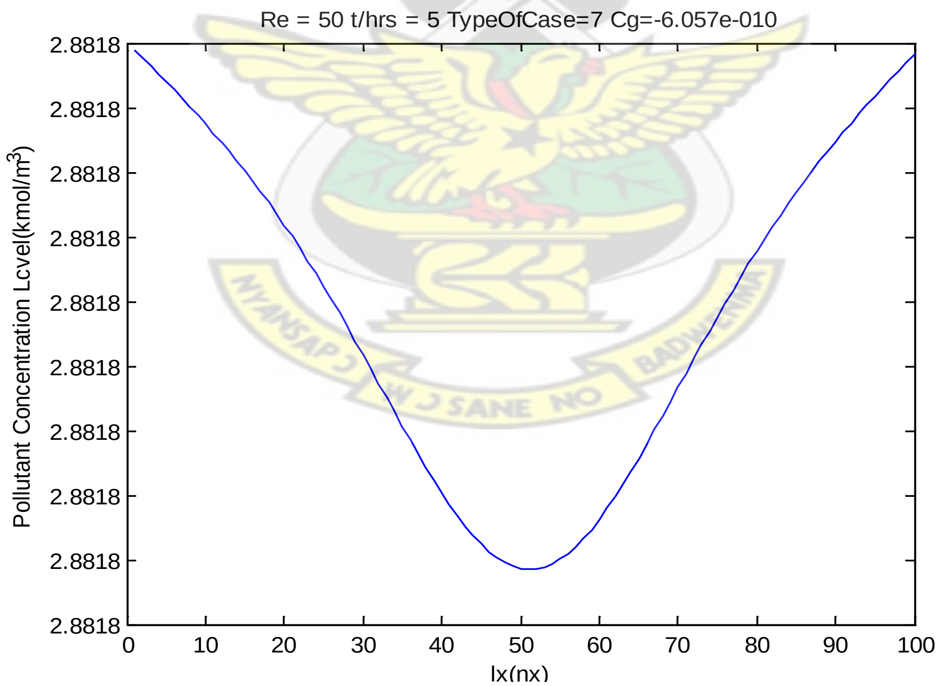

(b)

Figure 4.17: Concentration Profile along the Mid-point of lz-axis for case 7 with;

(a) Re=10 and (b) Re=50.

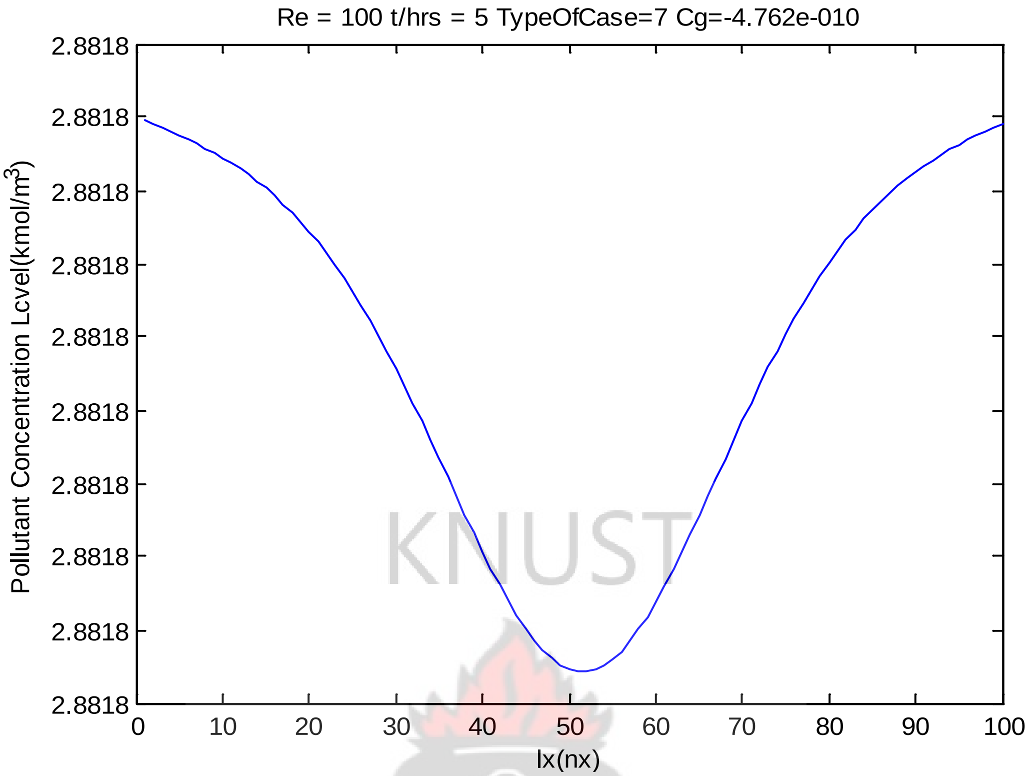

Figure 4.18: Concentration Profile along the Mid-point of lz-axis for case 7 with Re=100

Geometrically, the curved generated in Figures 4.15 to 4.18 for cases 6 and 7 above appear like an enlarged U-shape and V-shape respectively. For each of cases 6 and 7, the respective U and V shapes tend to gradually distort as the Reynolds numbers increase from 10 to 50 and to 100. Numerical analysis of both cases, reveal that the concentration levels (C) of the pollutant were found be relatively constant at a value of C= 2.8818 kmol/m^3. However, the slope of case 6 (Figures 4.15 to 4.16) rose gradually from Cg = -1.725×10^{-11} kmol/m^3 at Re=10 to Cg = -2.087×10^{-10} kmol/m^3 at Re=100. Similarly, that of case 7 (Figures 4.17 to 4.18) rose quite sharply from Cg =-6.192×10^{-11} kmol/m^3 at Re=10 to Cg =-4.762×10^{-10} kmol/m^3 at Re = 100. These confirm that the higher the Reynolds number for the same quantum of pollutant concentration at fixed source, the more swift as well as irregular and haphazard the distribution and dispersion of that pollutant.

4.5 The Impact of Time on Pollutant Distribution

Another parameter that has an influence on the rate of pollutant travel in a medium is time interval. In Figures 4.19 to 4.24 illustrated below, it is evident that the slopes of concentration levels (Cg) determined in all graphs show the existence of a constant concentration rate of distribution with times; t=0.5,1,3 and 5 (hours) for both cases 6 and 7. The longer the time interval, the higher the concentration levels along the midpoint of lz as more moles of the pollutant are able to disperse and travel to the midfield of the computational domain.

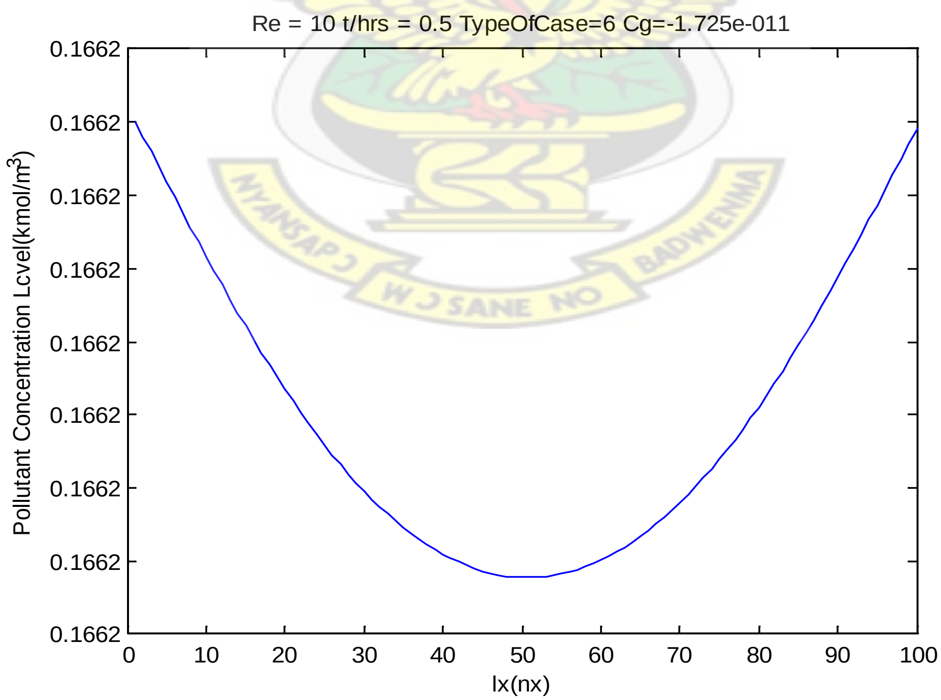

Figure 4.19: Concentration Profile along the Mid-point of lz-axis for case 6 with t=0.5

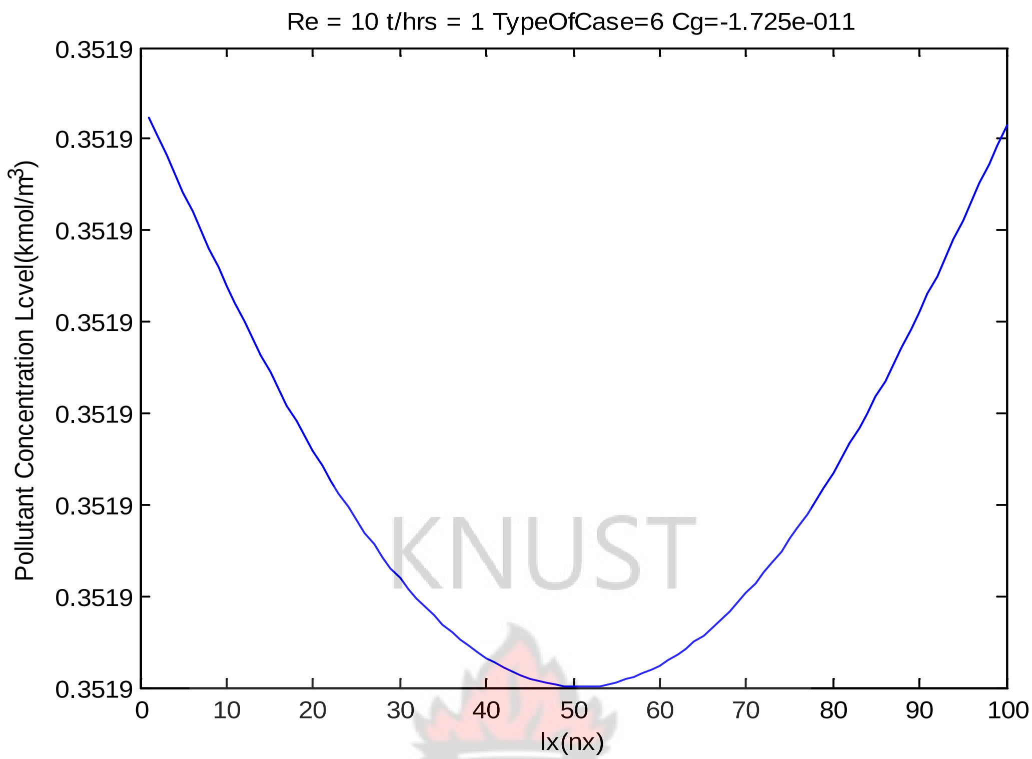

(a)

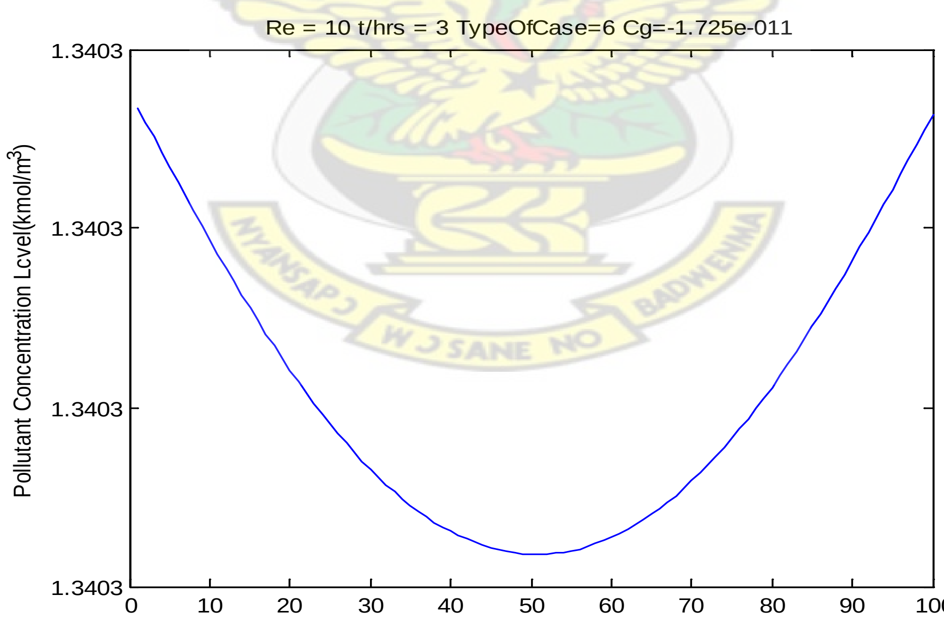

(b)

Figure 4.20: Concentration Profile along the Mid-point of lz-axis for case 6 with;

(a) t = 1and (b) t = 3

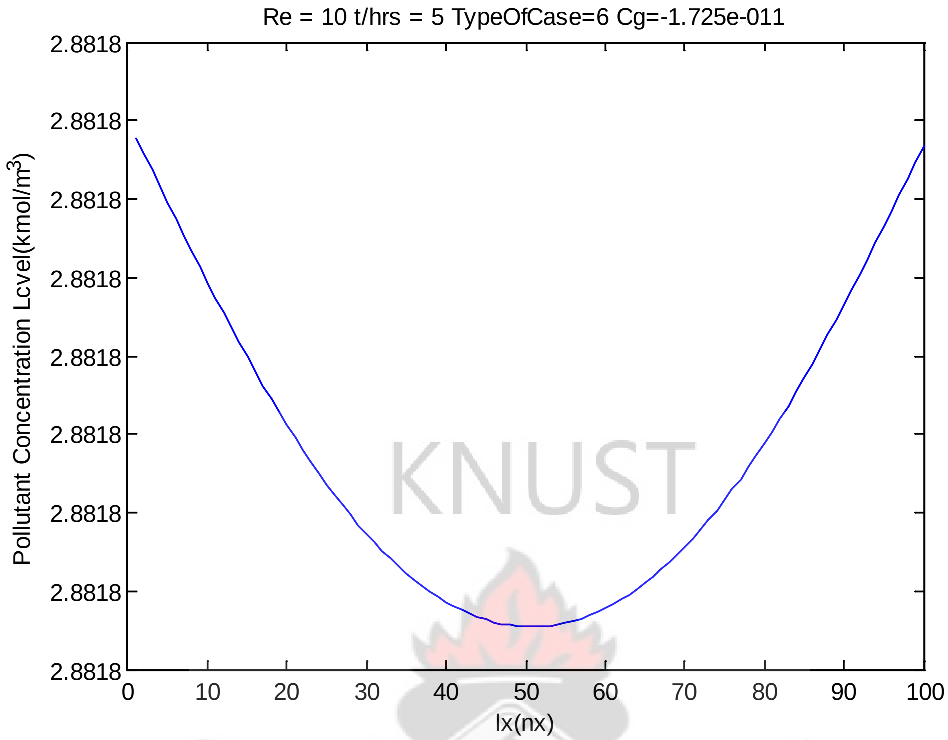

Figure 4.21: Concentration Profile along the Mid-point of lz-axis for case 6 with t=5

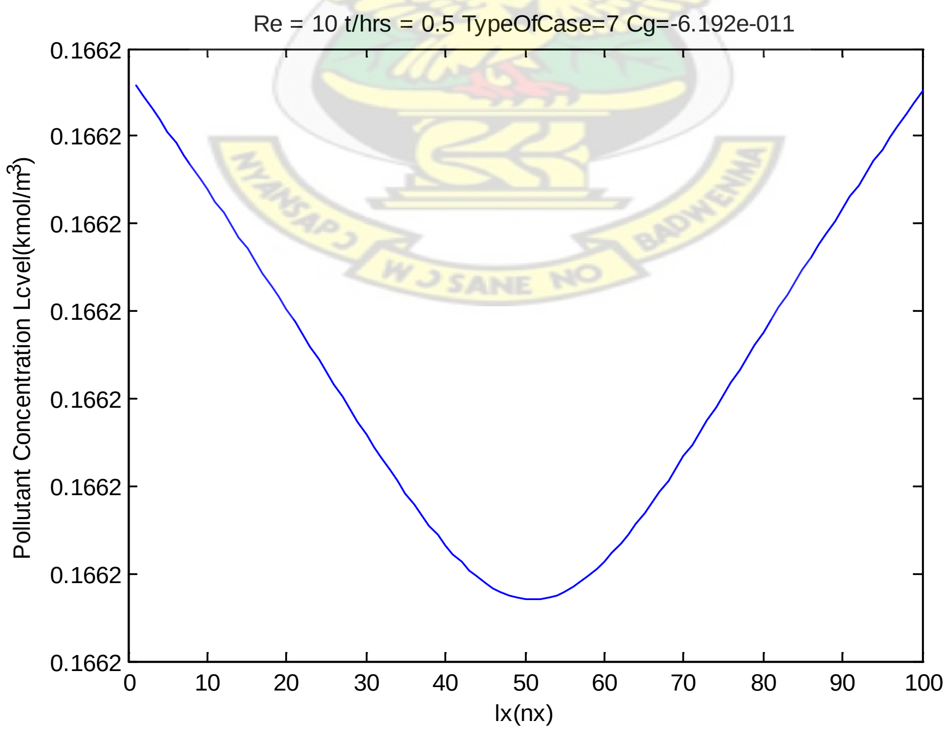

Figure 4.22: Concentration Profile along the Mid-point of lz-axis for case 7 with t=0.5

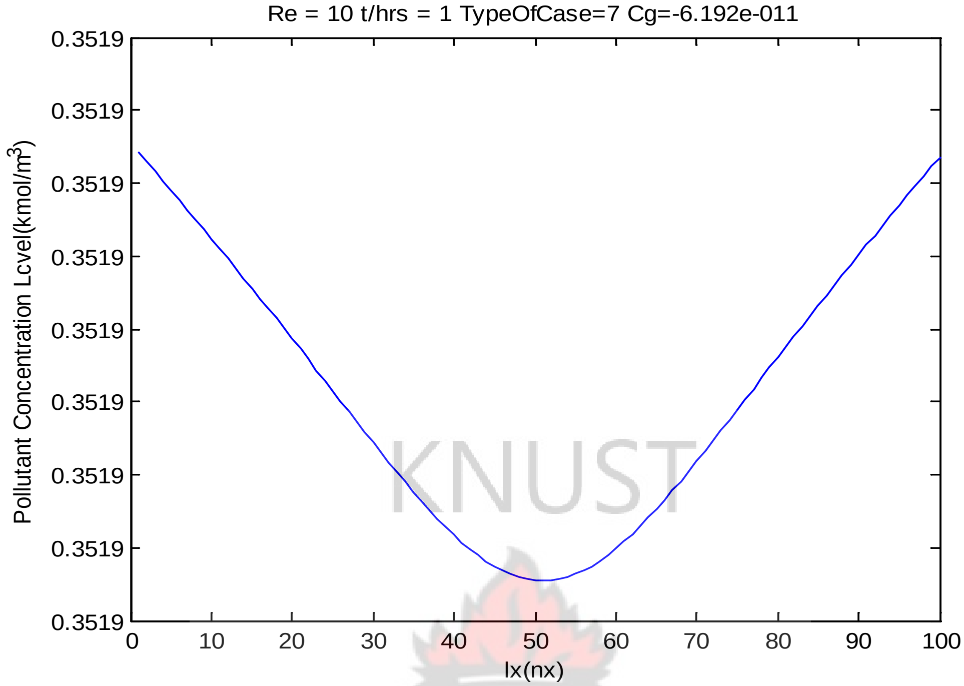

(a)

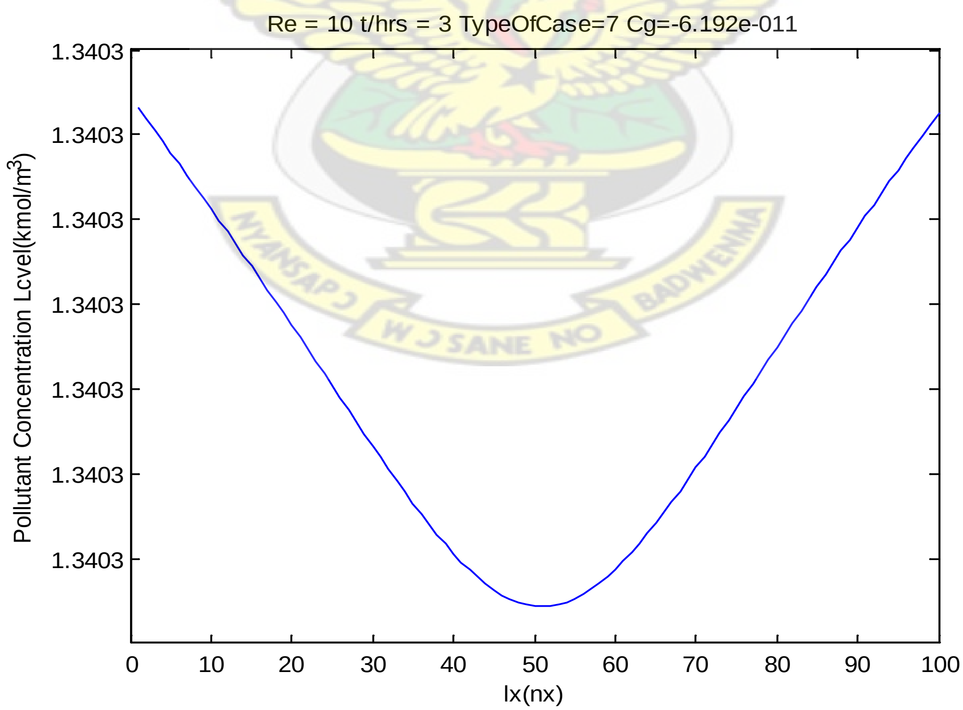

(b)

c

Figure 4.23: Concentration Profile along the Mid-point of lz-axis for case 7 with;

(a) t=1 and (b) with t=3.

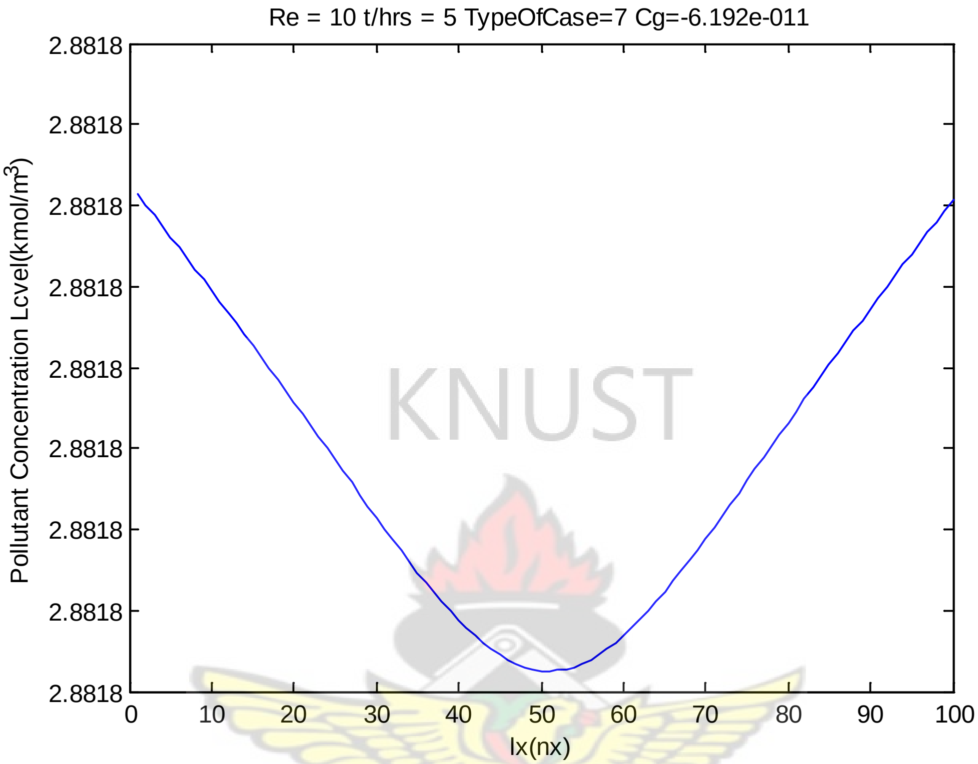

Figure 4.24: Concentration Profile along the Mid-point of lz-axis for case 7 with t=5

In both cases considered, the gradients (Cg) of the various curves remain constant at all times with Cg = -1.725 $\times 10^{-11}$ kmol/m^3 and Cg = -6.192 $\times 10^{-11}$ kmol/m^3 for case 6 and 7 respectively. Therefore, the rate of pollutant distribution depends on the pollutant travel time as well as the case under consideration or the source of the pollutant and its boundary conditions attached. This is because at equal times for cases 6 and 7, equal concentration levels were recorded but with different dispersion pattern. Moreover, the higher the pollutant travel time the higher the concentration level from a source to the fixed point under monitoring.

4.6 Experimental Results for Validation

The experimental results obtained for the three different cases considered were capture in four different time intervals. The photographs are shown in Figure 4.25 through to Figure 4.33. These figures represent the photographs captured during the experiment at various stages; the initial stage, after 30 minutes, after 1 hour, after 3 hours and after 5 hours consecutively for cases 3, 6 and 7.

Figure 4.25: Experimental set-up for the simulation of blue dye solution flowing through fine sand at initial stage to validate case 3.

(a)

(b)

Figure 4.26: Experimental set-up for the simulation of blue dye solution flowing through fine sand; (a) after 30 minutes and (b) after 1 hour to validate case 3.

(a)

(b)

Figure 4.27: Final flow pattern of Red dye solution flowing through fine sand;

(a) after 3 hours (b) after 5 hours to validate case 3.

(a)

(b)

Figure 4.28: Experimental set-up for the simulation of Red dye solution flowing through fine sand; (a) at initial stage and (b) after 30 minutes to validate case 6.

(a)

(b)

Figure 4.29: Experimental set-up for the simulation of Red dye solution flowing through fine sand; (a) after 1 hour and (b) after 3 hours to validate case 6.

Figure 4.30: Final flow pattern of Red dye solution flowing through fine sand after 5 hours to validate case 6.

(a)

(b)

Figure 4.31: Experimental set-up for the simulation of Red dye solution flowing through fine sand; (a) at initial stages and (b) after 30 minutes to validate case 7.

(a)

(b)

Figure 4.32: Experimental set-up for the simulation of Red dye solution flowing through fine sand after 3 hours to validate case 7.

Figure 4.33: Final flow pattern of Red dye solution flowing through fine sand after 5 hours to validate case 7.

It could be stated clearly that figures 4.27(b) , 4.30 and 4.33 truly confirms and validate the computer results obtained in Figures 4.5 and 4.6, Figure 4.11 and 4.12 that of Figure 4.13 and 4.14 respectively. This is because the flow pattern and configuration of the simulated results and experimental results are very similar. Hence, there is a positive correlation between the simulated results and experimental results.

CHAPTER 5

CONCLUSION AND RECOMMENDATION

5.1 Conclusion

Two dimensional flow of a water soluble pollutant through fine sand has been developed. The code which is a modified adapted Navier-Stokes equation for porous flow is used to simulate how water soluble pollutants manoeuvre their way through homogenous soil and any other homogeneous porous media. Several graphs plotted under section 4.2, 4.3 and 4.4 all point to the common assertion that there is an outstanding relation between the flow pattern (distribution and dispersion of pollutant) and the flow variables. This is more comprehensible when the concentration levels along the midpoint of the computational domain were determined and analyzed at varying Reynolds numbers and times using plotted curves (in Figures 4.15 to 4.24).

The gradients of the curves obtained (in Figures 4.15 to 4.18) were found to increase as Reynolds numbers increase for relatively constant pollutant concentration level within the same pollutant travelling time. However, at a constant Reynolds number the gradient of the curves remained relatively constant as time increases and with increasing concentration levels. Thus, at equal time intervals the concentration of the pollutant would generally disperse and distribute in a non-uniform manner at a rate proportional to the velocity (Reynolds number) of flow. In addition, at constant velocity (Reynolds number) the concentration of pollutant would generally disperse and distribute uniformly at a rate proportional to time interval.

The code was validated qualitatively using an experimental set-up performed by physically monitoring the flow of a dye from three different sources within a 2-m square by 3-cm depth of fine sand spread over a water proof carpet on a level ground. The distribution and dispersion pattern of the dye used was then physically examined at various times as simulated in the code and results compared. It was found that the concentration of the dye qualitatively decreased away from the source. This is evident from the physical analysis and observation of the dye configuration obtained at the end of all the three experiments. It has been established that water soluble pollutants travel uniformly through homogenous soil from a source to a sink as their concentration level from the source to the fixed point under monitoring also increases qualitatively with time. The higher the Reynolds number (velocity) of the flow, the higher the rate of pollutant distribution from the source to that fixed point(s) being monitored. Additionally, pollutants disperse in concentric shapes from their sources to sinks.

The analysis of the result shows that there is a very good level of agreement between the experimental and simulated results obtained. In conclusion, the model developed can be considered to be a good representation of the phenomenon of mobility of pollutants in the soil.

5.2 Recommendations

The following recommendations are necessary for future researchers:

1. Future codes should accommodate obstacle or non-permeable and non-homogenous medium in the computational domain. Within the soil layers may be found obstacles such as hardened rocks, concrete wall or moulds or sometimes metallic moulds and confinements. When situation of this nature is encountered, the problem becomes quite tougher as the pollutant would not be able to permeate through such obstacle but it is likely to move around the obstacle. Accordingly, the usual pollutant concentration level at and after the obstacle would possibly change entirely.
2. A wide variety of experimental models with different soil types should be built and results harmonized with simulated results. The soil is a mixture of different soil grades and it is appropriate to examine the behavior of the soluble pollutants through each soil type and probably that of a mixture of these soil types.
3. Reverse coding can be developed for tracing pollution sources. Most of the time, water soluble pollutants are discovered in an area or underground water without

knowing it exact source. A code could be developed so that it would be used to trace pollutant sources.

4. Three dimensional models should be designed to solve more challenging and compelling real life porous flow problems. This is necessary because, most porous flow problems that need be investigated and solved are in three dimensional configurations.

5.3 Limitations

The following constraints were encountered in the course of the research work:

1. There was inadequate and unreliable apparatus available to measure quantitatively the concentration levels at various points within the horizontal 2-metre square area of the experimental model. Hence the validation was done qualitatively by monitoring the concentration of dye colour at different time intervals.
2. At the geotechnical laboratory, there was no specific instrument that could be used to measure the porosity of the fine sand. Moreover, there are different empirical methods and formulae for computing the porosity of a soil sample. These formulae utilize some geotechnical parameters that depend on soil properties obtained at the laboratory. Since, different formulae and or methods may tend to give quite different results and this makes validations of simulated results somewhat questionable. This is because the correlation between experimental and simulated results may depend on the type of formula and method used.
3. There was the need to incorporate a three dimensional model but because of time constraints it could not be realized. Moreover, the computer cannot simulate a 3-D

model fully but analogous results may be obtained by chronological combination of several 2-D panels of a 3-D model.

REFERENCES

1. Analysis of Soil Heavy Metal Pollution and Pattern in Central Transylvania, (2008, April).
2. Bennethum, S. L. and Giorgi Tizian (1996). Generalized Forchheirmmer Equation for Two-Phase Based on Hybrid Mixture Theory. [http://wwwmath.ucdenver.edu/ccm/reports/rep092.pdf], (accessed 2010, September 23)
3. Clinton C. Truman and Donald P. Franzmeier. Structure, Pedological Concepts, and Water Flow.
4. Conceptual Models of Flow and Transport in the Fractured Vadose Zone (2001) Commission on Geosciences, Environment and Resources (CGER) (accessed 2009, December 14)
5. Cornell's Master of Professional Study Program in Integrated Watershed Management and Hydrology at Bahir Dar University, Ethiopia.(2009),[http:// soilandwater.bee.cornell.edu/Research/international/eth], (accessed 2009, September 11)
6. Dorea Felipe T. and Marcelo de Lemos J.S. (2010). Simulation of laminar pumping jet on porous medium . [http://www.sciencedirect.com/science?_ob=mimg&_

download/fahey/.../Permeabiity%20Notes.doc], (accessed 2010, September 22)

7. Droppo I. G. , Walling D. E. And Ongley E. D. (2000). The influence of floe size, density and porosity onsediment and contaminant transport [http://iahs.info/redbooks/a263/iahs_263_0141.pdf], (accessed, 2011, March 3rd)

8. Duijn van C. J., Eichel H., Helmig R, and Pop I. S. Effective equations for two-phase flow in porous media: the effect of trapping at the micro scale. [http://www.win.tue.nl/analysis/reports/rana05-34.pdf], (accessed 2010, September 23)

9. Effective equation for two phase flow in porous media [http://www.win.tue.nl/analysis/reports/rana05-34.pdf], (accessed 2010, September 23)

10. Flow equations in porous media [http://echo2.epfl.ch/vicaire/mod_3/chapt_6/], (accessed 2010, September 23)

11. Flow of water through soils. [140.194.76.129/publications/eng-manuals/em1110-3-136/c-4.pdf], (accessed 2010, September 23)

12. Gent Van M.R.A. (1992), Communications on hydraulic and geotechnical engineering, Formulae to describe porous flow;: 47.

13. Good, L. Ward and Madison, F. W. (1987). Soils of Portage County and Their Ability to Attenuate Contaminants. University of Wisconsin Extension and Wisconsin Geological and Natural History Survey

14. Grain size distribution and soil particle characteristic. [http://www.engineering.uiowa.edu/~swan/courses/53030/notes/gsd.pdf], (accessed 2010, September 23)

15. Hassanizadeh,M. and Gray,W.G.,(1979a).General conservation equations for multi-phase systems: 1.averaging procedure. AdvancesinWaterResources,2(3):131{ 144

16. Hassanizadeh, M. and Gray,W.G.,(1979b).Generalconservationequationsformulti-phase systems: 2. mass, momenta, energy, and entropy equations. Advances in Water Resources, 2(4):191{203.

17. Incompressible Fluids. [http://www.stanford.edu/class/me469b/handouts/ incompressible.pdf], (accessed 2010, September 2)

18. IRIN News East Africa: Lake Victoria Degradation Threatening Livelihoods, (accessed 2008, August 1).

19. IRIN. (2009). Raw sewage dumping a public health "time bomb" [http://www.irinnews.org/report.aspx?reportid=59809],(accessed 09 September 2009)

20. John D. Anderson, Jr. (1995). Computational Fluid Dynamics

21. K.R. Rushton (2003), Groundwater Hydrology; Conceptual and Computational Models.

22. Karheinz Spitz and Joanna Moreno. A practical guide to groundwater and solute transport modeling. (accessed 2009, August 8).

23. Koovevaar, P., Menelik, G., and Dirksen, C., (1983). Elements of Soil Physics. Developments in Soil Science. Elsevier, Amsterdam, third edition. ISBN 0-444-42242-0.

24. Macroscopic equations for flow in unsaturated porous media [http://www.mhoffmann.dds.nl/publications/hoffmann2003a.pdf] , (accessed 2010, September 23)

25. Milton Taylor D. (2003). Pesticide residues in coastal tropical ecosystems: distribution, fate and effects; : 19.

26. Miyazaki. Water flow in Soils, Second Edition.

27. Nick Price [a] and Qasim Chaudhry (2008) , QSAR Based Computational Models as Decision Making Tools in Bioremediation [http://www.technologyforgrowth.co.uk/cms_site/?q=node/78], (accessed, 2011, March 6th)

28. Papp,B., (2006).Method for determination of soil permeability by radon concentration measurement. [http://ion.elte.hu/~pappboti/kutatas/cikkek/enp6.pdf], (accessed 2010, September 22)

29. Partial Differential Equations in Matlab. [http://www.scribd.com/doc/2071569/partial-differential-equations-in-matlab], (accessed 2010, September 22)

30. Porosity and permeability. [http://research.ce.udel.edu/~imhoff/cieg337/assignments/2-hyd_cond_08_v2.pdf] , (accessed 2010, September 22)

31. Prevention of Water Pollution. [http://www.squidoo.com/PreventWaterPollution], (accessed 2009, June 20)

32. Principles of Soil physics, [http://cedb.asce.org/cgi/WWWdisplay.cgi?0003417], (accessed 2009, September 11)

33. Prof. Fahey Martin, Water flow in the Soil: Permeability [http://w2.civil.edu.au/

34. Public Agenda Ghana: Mine Company Accused of Leaking Poison into River, (accessed 2008, July 21).

35. S.P.G. Madabhushi, D. Bellotti, A.Clematis and P. Fernandes. (1988). Parallelisation of a Finite Difference Code for Modelling Ground Water Flow. (accessed 2009 , August 8).

36. Saturated Hydraulic Conductivity: Water Movement Concepts and Class History

37. Seepage flow and thermal effects in rigid porous media

38. Shao Aijun, Peng Jianping and Zhang Yongqiang (1999). Experimental Determination of Coefficient of Soil Hydrodynamic Dispersion [http://old.cgs.gov.cn/zt_more/34/zhaiyao/html/02/212.htm], (accessed, 2011, March 6th)

39. Soil pore size determination. [http://www.newton.dep.anl.gov/askasci/env99/ env201.htm], (accessed 2010, September 23)

40. Sonia Wouldberg (2006). Laminar Flow through Isotropic Granular Porous Media

41. Taylor. Fluid dynamics.

42. The relationship between permeability coefficients and solids [http://www. cti.uconn.edu/chwrp/pdfs/jhr88_180-86-5.pdf], (accessed 2010, September 23)

43. V. Viman, L. Mihaly Cozmuta, A. Mihaly Cozmuta, Gh. Vatca, C. Varga and G. Oprea (2005) Mathematical Modelling of Pollutants' Dispersion in Soil

[http://www.scipub.org/fulltext/ajes/ajes12126-129.pdf], (accessed, 2011, March 6th)

44. Water bodies in Obuasi and Tarkwa Poisioned. [http://www.modernghana.com/news/233810/1/water-bodies-in-obuasi-and-tarkwa-poisoned.html], (accessed 2009, September 9)
45. Water pollution causes. (2005). [www.grinningplanet.com], (accessed 2009, July 7)
46. Zeki Camur M. and Hasan Yazicigil (2001), Experimental determination of hydrodynamic dispersion coefficients for heavy metals using compacted clay [http://iahs.info/redbooks/a269/iahs_269_0283.pdf] , (accessed, 2011, March 6)
47. Soil and Water [http://soilandwater.bee.cornell.edu/Research/international/docs/Tilashwork%20Final%20thesis_formatted_review%20for%20printing.pdf], (accessed 2009, August 8)
48. Darcy's Law. [http://web.mit.edu/fluids-modules/www/porous_media/6-1darcy.pdf],(accessed 2010, September 23)
49. Reynolds Number. [http://www.engineeringtoolbox.com/reynolds-number-d_237.html],(accessed 2010, September 19)

APPENDIXES

APPENDIX I

MATLAB CODES FOR THE FLOW OF WATER SOLUBLE POLLUTANTS THROUGH SOIL

```
function modified_adapted_navierstokes_forporousflow
% Modified and Adapted Navier-Stokes equation for porous flow in the soil
% By Akowuah, Eric
%Postgraduate Student of the Mechanical Engineering Department ...
%Kwame Nkrumah University of Science and Technology (KNUST), Kumasi-Ghana.
%Under the Supervision of Dr. Joshua Ampofo of Mechanical Eng. Dept.,KNUST.
% E-mail: ek_akowuah2000@yahoo.com.sg
% Solves the incompressible Adapted Navier-Stokes equations in a
% computational domain with known velocities along the boundary.
% The solution method is finite differencing on a staggered grid with
% streamline plot for the velocity field and pollutant
% concentration field.
% Standard setup solves 2-dimensional contaminated water flow through soil.
 .........................................................................
% Definition of constants
.........................................................................
 g=9.81;  %acceleration due to gravity
 n=0.6;  %porosity of the soil
 rhof=1000; %density of the fluid/water
% meu=0.000798; %dynamic viscosity of water at 30 degree celsius
 meu=0.00065; %dynamic viscosity of oil polluted water
 v=meu/rhof;   % Kinematic viscosity
```

```
L=0.0002;        % pore characteristtic length scale( for fine sand)
K=0.03;  %intrinsic or absolute permeability of the soil
Re=linspace(0, 2.3e2,2.3e2+1);% Reynolds number range for laminar flow regime
for Re=input('Enter Reynolds number,Re=')
......................................................................
   % Definition  of coeficeints of adapted navierstokes equation
......................................................................
   if Re<1000
       Cd=24/Re*(1+0.15*Re^0.687);% Drag coefficient
   else
       Cd=0.44;
   end
end
Cm=0.975;     % Mass coefficient
Cl=0.067;         % Laminar coefficient( assumed)
ka=(1+Cm)/(n*g); % coefficient of advective term of the porous flow equations.
kc=(1+Cd)/(n^2*g); %coefficient of convective term
kp=1/(rhof*g); %coeffient of pressure term
kl=(Cl*v)/(g*L^2); % coefficient of laminar friction term
......................................................................
%Definition of pollutant parameters
......................................................................
kdc = 0.7;   % distribution coefficient(assumed)
Dl=0.65;      %Hydrodynamic dispersion coefficient(assumed)
rhob= 1.4;     %Solid density(assumed)
t =input('Enter pollutant dispersion time from source, t=');
......................................................................
% Defintion of the computational domain
......................................................................
lx =2;  % width of ....
%computational domain
```

```
lz =2; % depth of comptational domain
nx =100;% number of x-gridpoints
nz =100; % number of y-gridpoints
x = linspace(0,lx,nx+1);
dx = lx/nx; %grid cell width
z= linspace(0,lz,nz+1);
dz = lz/nz; %grid cell depth
.........................................................................
% Iterative conditions of flow
...........................................................................
nstps =10; % number of steps with graphic output
delta_t = 1e-2; % delta(t) for time step
delta_t = tf/nt
tf = 10e-0; % final time
nt = ceil(tf/delta_t);%number of time steps
U = zeros(nx-1,nz);
V = zeros(nx,nz-1);
.........................................................................
% Boundary conditions
...........................................................................
uSTH = x*0;
vSTH = mean(x)*0;
uWST = mean(z)*0;
vWST = z*0;
uEST = mean(z)*0;
vEST = z*0;
.........................................................................
% Other boundary conditions
...........................................................................
Uf=meu*Re/(4*rhof*sqrt(2*K/n)); %average filter velocity of fluid in the soil.
xp=Uf/sqrt(2)*ones(1,nx);
```

```
zp=Uf/sqrt(2)*ones(1,nz);
x0=x*0;
z0=z(1:nz)*0;
.........................................................................
% Type of case under consideration
.........................................................................
TypeOfCase=[1,2,3,4,5,6,7]; %10% pollutant coverage positions at the inflows
for TypeOfCase=input('Enter the type of case, TypeOfCase=')
  if TypeOfCase == 1;
 %Case 1; 10% pollutants coverage at the inflow and 90% pollutant free
 %of the North boundary length from West to East respectively
xp10 = xp(1:end-0.9*(nx));zp10=zp(1:end-0.9*nz);
xp90=x0(0.11*(nx):nx);zp90=z0(0.11*nx:nx);
uNTH0 = x*0+[xp10 xp90 0];
vNTH0 = mean(x)*0+[zp10 zp90];
       uNTH=uNTH0; vNTH = vNTH0;
   elseif TypeOfCase == 2;
 % case 2;10%pollutants coverage at the inflow in between 20% and 70% of
 % the North boundary length from West to East respectively
xp10=xp(0.21*nx:end-0.7*nx);
xp70=x0(0.31*nx:nx);
xp20=x0(1:0.2*nx);
uNTH20 = x*0+[xp20 xp10 xp70 0];
vNTH20 = mean(x)*0+[xp20 xp10 xp70];
        uNTH=uNTH20; vNTH=vNTH20;
   elseif TypeOfCase == 3;
  %case 3; 10% pollutants coverage at the inflow in between 40% and 50%
  % of the North boundary length from West to East respectively
xp10=xp(0.41*nx:0.5*nx);
xp40=x0(1:0.4*nx);
xp50=x0(0.51*nx:nx);
```

```
 uNTH40 = x*0+[xp40 xp10 xp50 0];
 vNTH40 = mean(x)*0+[xp40 xp10 xp50];
        uNTH=uNTH40; vNTH=vNTH40;
    elseif TypeOfCase == 4;
  % case 4; 10% pollutants coverage at the inflow in between 60% and 30%
   % of the North boundary length from West to East respectively
xp10=xp(0.61*nx:end-0.3*nx);
xp60=x0(1:0.6*nx);
xp30=x0(0.71*nx:nx);
uNTH60 = x*0+[xp60 xp10 xp30 0];
vNTH60 = mean(x)*0+[xp60 xp10 xp30];
        uNTH=uNTH60; vNTH=vNTH60;
    elseif TypeOfCase == 5;
  % case5; 10% pollutants coverage at the inflow in between 80% and 10%
   % of the North boundary length from West to East respectively
xp10=xp(0.81*nx:end-0.1*nx);
xp80=x0(1:0.8*nx);
xp100=x0(0.91*nx:nx);
uNTH80 = x*0+[xp80 xp10 xp100 0];
vNTH80 = mean(x)*0+[xp80 xp10 xp100];
        uNTH=uNTH80; vNTH=vNTH80;
    elseif TypeOfCase == 6;
  %Case 6;; 100% pollutants coverage at the inflow along the North boundary
 uNTHfull = x*0+Uf/sqrt(2)*ones(1,nx+1);
 vNTHfull = mean(x)*0+Uf/sqrt(2)*ones(1,nx);
        uNTH=uNTHfull; vNTH=vNTHfull;
   end
  if TypeOfCase == 7;
 %10% pollutants coverage at the centre of the computational domain with
 %fixed boundaries at N,S,E and W.
 uNTH=x*0;
```

```
 vNTH=mean(x)*0;
  end
     if TypeOfCase>7;
       disp('type of case does not exist, there are 1 to 7 cases')
     end
 end
 while TypeOfCase==7;
Ubc7=delta_t*(kl/ka)*([2*uSTH(2:end-1)' upx 2*uNTH(2:end-1)']/dx^2+...
    [uWST;zeros(nx-3,nz);uEST]/dz^2);
     xp10=xp(0.21*nx:end-0.7*nx);
     xp70=x0(0.31*nx:nx);
     xp20=x0(1:0.2*nx);
     uNTH20 = x*0+[xp70 xp10 xp20 0];
     vNTH20 = mean(x)*0+[xp70 xp10 xp20];
      up=uNTH20(1:end-3);
      px=zeros(nx-1,nz-2);
      pxx=zeros(1,nz-2);
      upx=[px(1:(nx-2)/2,1:end);up;px((nx-(nx-4)/2):end,1:end);pxx];
      vp=vNTH20(1:end-1);
      pz=zeros(nx-2,nz-1);
      vpz=[pz(1:(nx-2)/2,1:end);vp;pz((nx-(nx-2)/2):end,1:end)];
Vbc7 =delta_t*(kl/ka)*([vSTH' zeros(nx,nz-3) vNTH']/dx^2+...
      [2*vWST(2:end-1);vpz;2*vEST(2:end-1)]/dz^2);
 Ubc=Ubc7;
 Vbc=Vbc7;
 break
 end
 while TypeOfCase<7
 Ubc=delta_t*(kl/ka)*([2*uSTH(2:end-1)' zeros(nx-1,nz-2) 2*uNTH(2:end-1)']/dx^2+...
      [uWST;zeros(nx-3,nz);uEST]/dz^2);
Vbc =delta_t*(kl/ka)*([vSTH' zeros(nx,nz-3) vNTH']/dx^2+...
```

```
    [2*vWST(2:end-1);zeros(nx-2,nz-1);2*vEST(2:end-1)]/dz^2);
  break
 end
 ..........................................................................
% Generate interior matrices for U, V and P as well as the stream function
...........................................................................
fprintf('initialization')
Lp = kron(speye(nz),K1(nx,dx,1))+kron(K1(nz,dz,1),speye(nx));
Lp(1,1) = 3/2*Lp(1,1); perp = symamd(Lp); Rp = chol(Lp(perp,perp));
Rpt = Rp';
Lu = speye((nx-1)*nz)+delta_t/Re*(kron(speye(nz),K1(nx-1,dx,2))+...
    kron(K1(nz,dz,3),speye(nx-1)));
peru = symamd(Lu); Ru = chol(Lu(peru,peru)); Rut = Ru';
Lv = speye(nx*(nz-1))+delta_t/Re*(kron(speye(nz-1),K1(nx,dx,3))+...
    kron(K1(nz-1,dz,2),speye(nx)));
perv = symamd(Lv); Rv = chol(Lv(perv,perv)); Rvt = Rv';
Lq = kron(speye(nz-1),K1(nx-1,dx,2))+kron(K1(nz-1,dz,2),speye(nx-1));
perq = symamd(Lq); Rq = chol(Lq(perq,perq)); Rqt = Rq';
fprintf(', time loop\n--20%%--40%%--60%%--80%%-100%%\n')
for k = 1:nt
............................................................................
  % Treating the Convective term
............................................................................
   gamma = min(1.2*delta_t*max(max(max(abs(U)))/dx,max(max(abs(V)))/dz),1);
    Ue = [uWST;U;uEST]; Ue = [2*uSTH'-Ue(:,1) Ue 2*uNTH'-Ue(:,end)];
    Ve = [vSTH' V vNTH']; Ve = [2*vWST-Ve(1,:);Ve;2*vEST-Ve(end,:)];
    Ua = mean(Ue')'; Ud = diff(Ue')'/2;
    Va = mean(Ve); Vd = diff(Ve)/2;
    UVx = diff(Ua.*Va-gamma*abs(Ua).*Vd)/dx;
    UVz = diff((Ua.*Va-gamma*Ud.*abs(Va))')'/dz;
    Ua = mean(Ue(:,2:end-1)); Ud = diff(Ue(:,2:end-1))/2;
```

```
Va = mean(Ve(2:end-1,:)')'; Vd = diff(Ve(2:end-1,:)')'/2;
U2x = diff(Ua.^2-gamma*abs(Ua).*Ud)/dx;
V2z = diff((Va.^2-gamma*abs(Va).*Vd)')'/dz;
U = U-(kc/ka)*delta_t*(UVz(2:end-1,:)+U2x);
V = V-(kc/ka)*delta_t*(UVx(:,2:end-1)+V2z);
.....................................................................
% implicit viscosity
....................................................................
rhs = reshape(U+Ubc,[],1);
u(peru) = Ru\(Rut\rhs(peru));
U = reshape(u,nx-1,nz);
rhs = reshape(V+Vbc,[],1);
v(perv) = Rv\(Rvt\rhs(perv));
V = reshape(v,nx,nz-1);
....................................................................
% pressure correction
.....................................................................
p(perp) = -Rp\(Rpt\rhs(perp));
P = reshape(p,nx,nz);
Pp=reshape(P,1,nx*nz)';
rhs = reshape(diff([uWST;U;uEST])/dx+diff([vSTH' V vNTH']')'/dz,[],1);
U = U-(kp/ka)*delta_t*diff(P)/dx;
V = V-(kp/ka)*delta_t*diff(P')'/dz;
.....................................................................
% % stream function
.....................................................................
if floor(25*k/nt)>floor(25*(k-1)/nt), fprintf('.'),end
if k==1||floor(nstps*k/nt)>floor(nstps*(k-1)/nt)
    rhs = reshape(diff(U')'/dz-diff(V)/dx,[],1);
    q(perq) = Rq\(Rqt\rhs(perq));
    Q = zeros(nx+1,nz+1);
```

```
    Q(2:end-1,2:end-1) = reshape(q,nx-1,nz-1);
  end
end
.........................................................................
 % Finding the Final Velocity Profile with Laminar Resistance
.........................................................................
 U=reshape(U,1,(nx-1)*nz)'-(kl/ka)*delta_t*Uf/sqrt(2)*ones(1,(nx-1)*nz)';
 V=reshape(V,1,nx*(nz-1))'-(kl/ka)*delta_t*Uf/sqrt(2)*ones(1,nx*(nz-1))';
 U=reshape(U,nx-1,nz);
 V=reshape(V,nx,nz-1);
 Up=[zeros(1,nz);U];
 Vp=[zeros(nx,1),V];
 Upe= reshape(Up,1,nx*nz)';
 Vpe= reshape(Vp,1,nx*nz)' ;
 Vf=sqrt(Upe.^2+Vpe.^2+eps);
 Vt=reshape(Vf,nx,nz);
 .......................................................................
 % Computing the Pollutant concentration function
.........................................................................

   Cu=exp(t/(1+(kdc+rhob)/n))-exp((Up.*dx)/Dl);
   Cv=exp(t/(1+(kdc+rhob)/n))-exp((Vp.*dz)/Dl);
   Cup=reshape(Cu,1,nx*nz)';
   Cvp=reshape(Cv,1,nz*nx)';
   C=sqrt(Cup.^2+Cvp.^2+eps);
   Cp=reshape(C,nx,nz);
   C1=Cp(1:end,nz/2);
   C10=reshape(C1,1,nz);
   C50=reshape(C1,1,nz);
   C100=reshape(C1,1,nz);
   X=linspace(0,lx,nx);
```

```
   Z=linspace(0,lz,nz);
   FX=gradient(C10);
   Cg=(sum(FX)/nx);
fprintf('\n')
   .........................................................................
 % Displaying Flow Variables
...........................................................................
  format bank
  format long
  disp([Upe Vpe Vf Cup Cvp C ]) % Display The U-velocity Profile,
  %Prssure and Concentration profiles

............................................................................
 % Figure 1; Combined Plot for Flow Variables; velocity, Pressure,
%stream function and pollutant concentration
............................................................................
 figure(1),clf,contourf(mean(x),mean(z),Vt',20,'w-'),hold on
       contour(x,z,Q',20,'k-'), Lec = sqrt(Cu.^2+Cv.^2+eps);
       quiver(X,Z,(Cu./Lec)',(Cv./Lec)',.4,'k');colorbar;
     hold off, axis equal,axis([0 lx 0 lz]),
     Vt = sort(Vt); caxis('auto'); xlabel('lx'),ylabel('lz'),...
title(sprintf('Re = %0.3g t/hrs = %0.2g TypeOfCase=%0.1g'...
   ,Re,t,TypeOfCase)),
     drawnow ;
...........................................................................
 %Figure(2); Pollutanat Concentration plots, Stream function,
%velocity profile and pressure profile
 .........................................................................

figure(2),subplot(321),contourf(mean(x),mean(z),(Cu./Lec)',20,'w-');...
   xlabel('lx'), ylabel('lz'), title('Cu-Concentration in x-direction');
```

```
subplot(323),contourf(mean(x),mean(z),(Cv./Lec)',20,'w-');...
    xlabel('lx'), ylabel('lz'), title('Cv-Concentration in z-direction');
subplot(325),contourf(mean(x),mean(z),Cp',20,'w-');...
   xlabel('lx'), ylabel('lz'), title('Cp-Effective Concentration Profile');
subplot(322),contourf(x,z,Q',20,'w-');...
    xlabel('lx'), ylabel('lz'), title('Q-stream funtion');
subplot(324),contourf(mean(x),mean(z),Vt,20,'w-');...
    xlabel('lx'), ylabel('lz'), title('Vt-velocity profile');
subplot(326),contourf(mean(x),mean(z),P,20,'w-');...
    xlabel('lx'), ylabel('lz'), title('P-Pressure profile');
  % while TypeOfCase==7;
 while Re==10&&TypeOfCase==7||Re==10&&TypeOfCase==6;
 figure(3),plot(C10);
 xlabel('lx(nx)'), ylabel('Pollutant Concentration Lcvel(kmol/m^3)'),...
 title(sprintf('Re = %0.3g t/hrs = %0.2g TypeOfCase=%0.1g Cg=%0.4g'...
 ,Re,t,TypeOfCase,Cg)),
 break
 end
 while Re==50&&TypeOfCase==7||Re==50&&TypeOfCase==6;
  figure(4), plot(C50);
  xlabel('lx(nx)'), ylabel('Pollutant Concentration Lcvel(kmol/m^3)'),...
 title(sprintf('Re = %0.3g t/hrs = %0.2g TypeOfCase=%0.1g Cg=%0.4g'...
 ,Re,t,TypeOfCase,Cg)),
  break
 end
 while Re==100&&TypeOfCase==7||Re==100&&TypeOfCase==6;
  figure(5), plot(C100);
  xlabel('lx(nx)'), ylabel('Pollutant Concentration Lcvel(kmol/m^3)'),...
 title(sprintf('Re = %0.3g t/hrs = %0.2g TypeOfCase=%0.1g Cg=%0.4g'...
 ,Re,t,TypeOfCase,Cg)),
  break
```

```
end

function A = K1(n,h,a11)
% a11: Neumann=1, Dirichlet=2, Dirichlet mid=3;
A = spdiags([-1 a11 0;ones(n-2,1)*[-1 2 -1];0 a11 -1],-1:1,n,n)'/h^2;
function B = mean(A,k)
if nargin<2, k = 1; end
if size(A,1)==1, A = A'; end
if k<2, B = (A(2:end,:)+A(1:end-1,:))/2; else, B = mean(A,k-1); end
if size(A,2)==1, B = B'; end
```

APPENDIX II

DETERMINATION OF COEFFICIENT OF PERMEABILITY FOR FINE SAND

GEOTECHNICAL ENGINEERING LABORATORY
FALLING HEAD PERMEABILITY

PROJECT NAME: Determination of Coefficient of Permeability **Date:** 14th October, 2010

SAMPLE: Fine Sand

Diameter of Sample	**cm**	10.50
Diameter of Standpipe	**cm**	1.00
Area of Sample	**cm^2**	86.60
Area of Standpipe	**cm^2**	0.78
Length of soil	**cm**	11.20
Adjustment height	**cm**	91.80

Test		**1**	**2**	**3**
Initial Water level in the pipe	**cm**	89.0	90.0	94.0
Final water Level in the pipe	**cm**	69.5	73.1	76.7
Time Elapsed (t)	**sec**	1800	1800	1800
Initial head of water in the pipe	**h_0**	180.8	181.8	185.8
Final head of Water in the pipe	**h_1**	161.3	164.9	168.8
h_0/h_1		1.1209	1.1025	1.1027
$2.3\log(h_0/h_1)$		0.114004	0.097471	0.097651
Permeability (k)	**cm/sec**	6.4344×10^{-6}	5.5013×10^{-6}	5.5114×10^{-6}
Average Permeability (k)	**cm/sec**	**5.8157×10^{-6}**		

APPENDIX III

WORKPLAN

Year: 2009-2010	Month	July-Aug		Aug-Sept		Oct-Nov		Nov-Dec		Dec-Jan	
Activity	Week	First-third	4th-6th	7th-9th	10th-12th	13th-15th	16th-18th	19th-21st	22nd-24th	25th-27th	28-30th
1. Literature review											
2. Study of ground water flow											
3. Revising CFD equations in connection with water flow											
4. learning relevant programming software											
5. developing algorithm for the program											
6. writing codes for the program											
7. Discussion and Validation of Results											
8. Submission of Thesis											

APPENDIX IV

BUDGET

NO.	ACTIVITY	DETAILS OF ACTIVITY	UNIT COST(GH¢)	SUB-TOTAL (GH¢)
	1.0 Literature review	1.1 Photocopies at libraries	0.05 per copy	0.05×500 =25
		1.2Visiting commercial Internet facilities	0.7 per hour	0.7 ×50 =35
2	2.0 Studying water flow	2.1 Learning Materials from bookshops	30 per book	30×3 =90
		2.2 Visit internet facilities	0.7 per hour	0.7 ×50 =35
3	3.0 Revising CFD equations.	3.1 Purchase of CFD books	50 per book	50×2=100
		3.2 Search for current equations from the internet	0.7 per hour	0.7 ×30 =21
4	4.0 Programming Software	4.1 Purchase of Visual Basic software	90 per book	90
		4.2 Purchase of MATLAB software	200 per disc	200
5	5.0 Developing Algorithm for the program & coding	5.1T&T for consultations	5 per day	8×5= 40
		5.2 Writing and coding	3 as allowance per day	20×3=60
6	6.0 Validation of Results	6.1 Searching for standard data	10 per T&T	5×10= 50
		6.2 Setting up practical illustration for validation	5 as allowance per day	5×8=40
			SUM TOTAL(GH¢)	786.00
			MISCELLANEOUS (10% OF SUM TOTAL)	78.60
			GRANDTOTAL (GH¢)	864.60

TABLE OF CONTENT

Contents **Page**